# Lattice model of equilibrium polymerization. IV. Influence of activation, chemical initiation, chain scission and fusion, and chain stiffness on polymerization and phase separation

Jacek Dudowicz and Karl F. Freed[a)]
*The James Franck Institute and the Department of Chemistry, The University of Chicago, Chicago, Illinois 60637*

Jack F. Douglas
*Polymers Division, National Institute of Standards and Technology, Gaithersburg, Maryland 20899*

(Received 5 August 2003; accepted 19 September 2003)

The influence of thermal activation, chemical initiation, chain fragmentation, and chain stiffness on basic thermodynamic properties of equilibrium polymerization solutions is systematically investigated using a Flory–Huggins type lattice model. The properties treated include the average chain length $L$, extent of polymerization $\Phi$, Helmholtz free energy $F$, configurational entropy $S$, specific heat $C_V$, polymerization transition temperature $T_p$, osmotic pressure $\Pi$, and the second and third virial coefficients, $A_2$ and $A_3$. The dependence of the critical temperature $T_c$ and critical composition $\phi_c$ (volume fraction of associating species) on the enthalpy $\Delta h_p$ and entropy $\Delta s_p$ of polymerization and on the strength $\epsilon_{\mathrm{FH}}$ of the FH effective monomer–solvent van der Waals interaction ($\chi=\epsilon_{\mathrm{FH}}/T$) is also analyzed as an illustration of the strong coupling between phase separation and polymerization. For a given polymerization model, both $T_c$ and $\phi_c$, normalized by their values in the absence of polymerization, are functions of the dimensionless ''sticking energy'' $h_\epsilon \equiv (|\Delta h_p|/R)/(2\epsilon_{\mathrm{FH}})$ (where $R$ is the gas constant) and $\Delta s_p$. © *2003 American Institute of Physics.* [DOI: 10.1063/1.1625642]

## I. INTRODUCTION

Our recent series of papers[1–3] stresses that the general nature of the thermodynamic properties of reversibly associating particle and molecular systems can be inferred from the behavior of the classic example of ''living polymerization'' in solution. This focus on living polymerization is dictated by the availability of careful measurements for this type of complex fluid[4,5] and by the relative simplicity of the underlying mean field theory that restricts itself to chain growth occurring exclusively at the chain ends due to the presence of a chemical ''initiator.'' Of perhaps more far reaching implications, we have argued[1–3] that this model is generally representative of other associating particle systems because the equilibrium condition should make the details of chain connectivity and the mode of cluster growth and fragmentation of secondary significance in mean field theory. While much physical evidence supports these arguments, it remains to establish the correctness of this ''universal'' view of the thermodynamics of equilibrium particle clustering through the systematic treatment and comparison with other models for equilibrium polymerization in which there are different constraints on the polymerization process. These different constraints are very relevant to descriptions of clustering in complex fluids that polymerize without the presence of chemical initiators, which are essential components of the model analyzed in Papers I–III. In particular, we focus in this paper on the influence of activation, chemical initiation, and chain stiffness on the general thermodynamic properties of equilibrium polymer solutions and, specifically, on the competition between chain formation and phase separation. A subsequent paper will describe how constraints on chain topology (i.e., branching) affect the same thermodynamic and critical properties.[6]

Dynamic clustering of atomic and particle systems at equilibrium is ubiquitous in nature,[1] and consequently numerous studies have emphasized various aspects of this phenomenon since the pioneering work of Dolezalek[7] nearly a century ago. Fisher and Zuckerman[8] review the evolution, impact, and difficulties in modeling this type of association phenomenon in the context of ionic solutions where the presence of clustering has long been appreciated. Gee[9] and Tobolsky and Eisenberg[10,11] made pioneering contributions to modeling the equilibrium polymerization of linear polymer chains, and the history of this topic is summarized by Petschek *et al.*[12] and Greer.[4,5] Associating fluids are also extensively discussed in the chemical engineering literature. For example, Economou and Donohue[13] discuss the use of integral equation theories for associating fluids and the interrelations between chemical association models of these fluids. Highly informative simulations of equilibrium polymerization by Jackson *et al.*[14] and Milchev and co-workers[15,16] are also notable. The influence of fluctuations on the critical behavior of activated and initiated equilibrium polymers has been investigated by Wheeler and co-workers,[17–22] and Cates and co-workers[23,24] present scaling arguments indicating how excluded volume interactions affect chain properties.

Our studies of equilibrium polymerization owe a particu-

[a)]Electronic mail: k-freed@uchicago.edu

 

lar debt to Tobolsky and Eisenberg[10,11] and Scott[25] who introduce a general classification scheme into their modeling of equilibrium polymerization and the competition between phase separation and chain association in activated polymerization systems. These early investigations focus on modeling the polymerization process in particular physical systems, such as sulfur,[25] and many basic aspects of the coupling between polymerization and phase separation remain to be investigated analytically. Given the importance of this type of model as a paradigm for molecular self-organization, there is a need for systematic investigation of how the general classes of polymerization (thermally activated, chemically initiated, and freely associating),[10] influence the critical solution properties $(T_c, \phi_c)$, the transition lines governing the location of the polymerization transition, and essential thermodynamic solution properties (osmotic pressure, theta temperature, second and third osmotic virial coefficients, etc.). This kind of information is required for identifying the mechanism of polymerization occurring in real systems and for determining the relevant interaction parameters governing these transitions. We are particularly interested in dynamic clustering in connection with understanding the thermodynamics and the stability of nanoparticle dispersions in polymeric materials, polyelectrolyte solutions, and colloid dispersions. Many aspects of the theory are developed here for future applications to these complex fluids, although these applications are not explicitly discussed in the present paper. For example, a separate paper[26] considers phase separation in associating dipolar fluids, and the free energy expression derived here is an important component of that work. Our comparative study of these associating fluids confirms the presence of certain general patterns in the thermodynamic properties, but also emphasizes the regulatory effect of the activation and chemical initiation processes on the average mass distribution of the polymers that are formed and on the breadth of the polymerization transition. We systematically investigate the impact of these ''constraints'' on the polymerization transition to resolve further which solution properties are ''universal'' or specific to a particular type of polymerization process.

Section II describes the simplest model of an associating fluid in which all monomers can associate with each other without either activation or chemical initiation. Section III summarizes the essential results for the thermodynamic properties of polymer solutions undergoing equlibrium polymerization controlled by an activation process. Notably, within the Flory–Huggins (FH) model,[27] the thermodynamic properties in both models of Secs. II and III are found to be completely insensitive to the mode of linear association (i.e., to whether the chains grow by adherence of monomers to the chain ends or by linking two chains at their ends and to whether the chains may break in the middle or lose terminal segments). The theoretical expressions for a wide range of thermodynamic properties are derived for the two extremes of chain semiflexibility, i.e., for fully flexible and stiff chains. The free association model of Sec. II is shown to emerge as a special case of the activated association model. For completeness, Sec. IV briefly reviews some basic thermodynamic characteristics of the chemically initiated equilibrium polymerization model (''living polymerization'') that is the subject of our earlier papers.[1–3] This review also includes some new results (e.g., third virial coefficient, asymptotic analysis of the critical temperature and critical composition, etc.). Section V provides a critical comparison of these basic equilibrium polymerization models.

Before developing the theory, we summarize some of the assumptions invoked. The treatment is based on a mean field FH lattice model description for the thermodynamics of these associating polymer solutions where the differences in the solvent and monomer structure are neglected and where the solutions are assumed to be incompressible. The equilibrium polymerization models developed here employ the minimal number of parameters necessary to distinguish between different classes of polymerization. Many possible extensions simply follow from improvements of the FH theory.[27] For example, structural differences between species can be treated using the lattice cluster theory generalization of the FH model.[28] We neglect orientational interactions that are important for semiflexble chains at higher concentrations.[29]

## II. "FREE ASSOCIATION" MODEL

The simplest possible model of equilibrium polymerization postulates that each molecule or particle can associate with another monomer or polymer chain. This polymerization model corresponds to case III in the general classification scheme of Tobolsky and Eisenberg[10] and is popular as an approximate model of worm-like micelles.[30] Recently, this model has also been used to describe dynamic clustering in ionic fluids comprised of ions and counterions of highly disparate sizes.[31]

The system studied is composed of $n_s$ solvent molecules and $n_1^o$ monomers of species $M$ that can ''freely associate'' into polymers once the free energy of this association process becomes negative. The resulting polymers form and disintegrate in dynamic equilibrium, and attention is confined to the time-averaged properties of these complex fluids.

The free association model places no restrictions on the mechanism of chain formation and disintegration, so that chain growth may proceed by addition of a single monomer or by the linkage of two chains. Similarly, chains may break in the middle, or segments may dissociate from the chain ends. The two modes of polymerization can be characterized by the single kinetic equation,

$$M_j + M_k \rightleftharpoons M_{j+k}, \quad j,k = 1,2,\ldots,\infty. \tag{1}$$

The numbers of molecules $\{n_i\}$ of the individual species $M_i$ are related to the initial number of monomers, $n_1^o$ by the mass conservation condition,

$$n_1^o = \sum_{i=1}^{\infty} i n_i. \tag{2}$$

The thermodynamic properties of the system are described using a minimal incompressible Flory–Huggins lattice model, where a single site occupancy constraint applies to solvent molecules and to all monomers (unreacted as well

as those in the polymers). Thus, the total number $N_l$ of lattice sites is written in terms of the numbers of molecules $\{n_i\}$ of the individual species $M_i$ as

$$N_l = n_s + \sum_{i=1}^{\infty} n_i i = n_s + n_1^o, \tag{3}$$

and the total Helmholtz free energy $F$ for the system is given by

$$\frac{F}{N_l k_B T} = \phi_s \ln \phi_s + \sum_{i=1}^{\infty} \frac{\phi_i}{i} \ln \phi_i + \phi_s \chi \sum_{i=1}^{\infty} \phi_i + \sum_{i=2}^{\infty} \phi_i f_i, \tag{4}$$

where $\phi_s = n_s/N_l = 1 - \phi_1^o$ and $\{\phi_i = n_i i/N_l\}$ denote the volume fractions of the solvent and of $i$-mers, respectively. $\chi = \epsilon_{\mathrm{FH}}/T$ is the dimensionless monomer–solvent interaction parameter, $f_i$ is the dimensionless specific free energy of an $i$-mer, and $k_B$ is Boltzmann's constant. For simplicity, all monomers are assumed to interact identically with the solvent molecules, regardless of whether they are unpolymerized or belong to polymerized species. Hence, the effective interaction parameter $\chi_{mm'}$ between unreacted monomers and the monomers in polymers is taken to vanish identically. The specific free energy $f_i$ is quoted in the following, while the quantities $f_1$ and $f_s$ are taken as vanishing identically since both solvent and monomer species are treated as entities occupying single lattice sites. The latter assumption implies, in turn, that the internal entropies of both solvent and monomer molecules define our zero of entropy, so that the entropies computed from Eq. (4) are *not* absolute quantities. The mass conservation constraints from Eq. (2) can be reexpressed conveniently in terms of volume fractions as

$$\phi_1^o = \sum_{i=1}^{\infty} \phi_i, \tag{5}$$

where $\phi_1^o = n_1^o/N_l$ is the volume fraction of monomers before polymerization.

The condition of chemical equilibrium imposes the relation between the chemical potentials $\mu_j$, $\mu_k$, and $\mu_{j+k}$ of the $M_j$, $M_k$, and $M_{j+k}$ species, respectively,

$$\mu_j + \mu_k = \mu_{j+k}, \quad j,k = 1,2,\ldots,\infty. \tag{6}$$

Equation (6) can be rearranged into the simpler relation

$$\mu_i = i\mu_1, \quad i = 2,3,\ldots,\infty. \tag{7}$$

that formally corresponds to the following sequential polymerization scheme:

$$M_i + M_1 \rightleftharpoons M_{i+1}, \quad i = 1,2,\ldots,\infty. \tag{8}$$

The equivalence of Eqs. (6) and (7) explicitly demonstrates that the equilibrium properties predicted by the free association model are *completely insensitive* to whether the chains grow by addition of single monomers to the chain ends or by linking two chains and whether they break at their ends or in the middle. In fact, this insensitivity is implicit in Eq. (1). The chemical potentials $\{\mu_i\}$ can be calculated directly from the free energy of Eq. (4) as

$$\mu_i - i\mu_s = \left.\frac{\partial F}{\partial n_i}\right|_{T,N_l,n_{k\neq i}}, \tag{9}$$

where the exchange chemical potential $\mu_i^{\mathrm{ex}} \equiv \mu_i - i\mu_s$ (with $\mu_s$ being the solvent chemical potential) emerges from Eq. (4) as a consequence of the assumed incompressibility of the system. After simple algebra, the equilibrium condition in Eq. (7) takes a form in which the $\mu_s$ terms cancel identically, leading to the simple result

$$\ln\left[\frac{\phi_i}{\phi_1^i}\right] = i - 1 - i f_i, \quad i = 2,3,\ldots,\infty. \tag{10}$$

It is possible within FH theory[27] to describe polymer chains as semiflexible molecules (as in Paper I[1]), but for notational compactness, we present the derivation for the two extreme limits of chain semiflexibility, i.e., for fully flexible chains and stiff rods. This specialization is chosen because the description of these two limits does not require introducing an additional parameter, i.e., the energy difference between *gauche* and *trans* conformations. The specific free energy $f_i$ $(i = 2,3,\ldots,\infty)$ is obtained from the Flory theory for linear, fully flexible polymer chains as

$$f_2 = \frac{1}{2}\ln\left[\frac{2}{2z}\right] + 1 - \frac{1}{2} + \frac{1}{2}\frac{\Delta f_p}{k_B T} \tag{11}$$

and

$$f_i = \frac{1}{i}\ln\left[\frac{2(z-1)^2}{iz}\right] + \frac{i-1}{i} - \ln(z-1) + \frac{i-1}{i}\frac{\Delta f_p}{k_B T}, \quad i \geqslant 3, \tag{12}$$

where $z$ is the lattice coordination number and $\Delta f_p$ designates the free energy change due to the polymerization reaction in Eq. (1), a modification appended to the Flory specific free energy in order to describe the free association system. The necessity of distinguishing between $f_2$ and $f_i$, $(i \geqslant 3)$ is obvious since dimers are not flexible objects. Consequently, the $f_2$ in Eq. (11) does not contain factors of $\ln(z-1)$ that reflect the flexibility of higher order polymers $(i \geqslant 3)$. In the limit where all polymers are modeled as stiff rods, Eq. (12) is replaced by

$$f_i = \frac{1}{i}\ln\left[\frac{2}{iz}\right] + 1 - \frac{1}{i} + \frac{i-1}{i}\frac{\Delta f_p}{k_B T}, \quad i \geqslant 2. \tag{13}$$

Combining Eqs. (10)–(13) leads to the compact expression for the volume fractions $\{\phi_i\}$,

$$\phi_i = iCA^i, \quad i \geqslant 2, \tag{14}$$

with the quantity $A$ given by

$$A \equiv \phi_1(z-1)K_p \quad \text{(fully flexible chains)}, \tag{15}$$

$$A \equiv \phi_1 K_p \quad \text{(stiff chains)}, \tag{16}$$

where $K_p = \exp(-\Delta f_p/k_B T)$ is the equilibrium constant for the polymerization reaction [see Eq. (1)] in the stiff chain system. A factor of $(z-1)$ in Eq. (15) can be absorbed into the definition of $\Delta s_p$ for the fully flexible chain model, but we retain Eq. (15) unchanged for clarity of comparison between systems of flexible and rigid chains. Thus, the equilib-

rium constant of reaction (1) in the fully flexible chain system is defined as the product of $K_p$ and $(z-1)$.

The prefactor $C$ for these two limits of chain stiffness has the corresponding definitions,

$$C \equiv \frac{z}{2(z-1)^2 K_p} \quad \text{(fully flexible chains)}, \tag{17}$$

$$C \equiv \frac{z}{2K_p} \quad \text{(stiff chains)}. \tag{18}$$

As shown above, the distribution of $i$-mers is insensitive to the monomer–solvent interaction parameter $\chi$ and is solely governed by the temperature, inital monomer concentration $\phi_1^o$, energy $\Delta h_p$, and entropy $\Delta s_p$ of polymerization ($\Delta f_p = \Delta h_p - T\Delta s_p$). The insensitivity of $\{\phi_i\}$ to the presence of weak van der Waals interactions no longer applies[32] when we distinguish between polymer–solvent and monomer–solvent interactions or assume a non-vanishing monomer–polymer interaction parameter $\chi_{mp} \equiv \chi_{mm'} \neq 0$.

Substituting Eq. (14) into Eq. (5) and performing all the summations (with the constraint $0<A<1$) yield the important relation between $\phi_1^o$ and $\phi_1$,

$$\phi_1^o = \phi_1 + \frac{CA^2(2-A)}{(1-A)^2}. \tag{19}$$

This nonlinear equation must be solved numerically to determine $\phi_1$ as a function of $T$ and $\phi_1^o$.

After inserting Eq. (14) and performing the summations in Eq. (4), the Helmholtz free energy $F$ for the system reduces to the following form:

$$\frac{F}{N_l k_B T} = (1-\phi_1^o)\ln(1-\phi_1^o) + \phi_1^o \ln \phi_1 + (1-\phi_1^o)\phi_1^o \chi + \frac{CA^2}{(1-A)^2}, \tag{20}$$

which specifies $F$ for a given set of parameters $T$, $\phi_1^o$, $\epsilon_{\mathrm{FH}}$, $\Delta h_p$, and $\Delta s_p$. (Note that $A$ is proportional to $\phi_1$.) The basic thermodynamic properties, such as internal energy $U$ (=enthalpy $H$ within an incompressible FH model), specific heat $C_V$ ($=C_P$), and entropy $S$ of the system follow from Eq. (20) as standard derivatives of the free energy $F$,

$$\frac{U}{N_l k_B T} = \frac{1}{N_l k_B T} \left.\frac{\partial [F/(k_B T)]}{\partial [1/(k_B T)]}\right|_{N_l} = (1-\phi_1^o)\phi_1^o \chi + \frac{CA^2}{(1-A)^2}\frac{\Delta h_p}{k_B T}, \tag{21}$$

$$\frac{S}{N_l k_B} = \frac{1}{N_l}\left.\frac{\partial F}{\partial T}\right|_{N_l} = -(1-\phi_1^o)\ln(1-\phi_1^o) - \phi_1^o \ln \phi_1 + \frac{CA^2}{(1-A)^2}\left[\frac{\Delta h_p}{k_B T} - 1\right], \tag{22}$$

and

$$\frac{C_V}{N_l k_B} = \frac{1}{N_l k_B}\left.\frac{\partial U}{\partial T}\right|_{N_l} = \left(\frac{\Delta h_p}{k_B T}\right)^2 \frac{2CA^2}{(1-A)^3}\left[\frac{\phi_1^o}{\phi_1^o + \frac{2CA^2}{(1-A)^3}} - \frac{1-A}{2}\right]. \tag{23}$$

Following conventional usage, the enthalpy of polymerization $\Delta h_p$ is called the "sticking energy." Equation (22) yields the entropy relative to that of unpolymerized monomers in solution rather than the absolute entropy, and, thus, this relative entropy may be negative. The polymerization transition temperature $T_p$ is defined by the maximum in the specific heat $C_V(T)$, and the variation of $T_p$ with $\phi_1^o$ is termed a "polymerization transition line." For systems that polymerize upon cooling, the monomers, generally, remain largely unpolymerized above $T_p$, while significant polymerization occurs for $T \leqslant T_p$. The reverse situation ensues for systems that polymerize upon heating. The interpretation of the polymerization line as a boundary between the monomer rich and polymer rich "phases" becomes less adequate when the polymerization transition is very broad, as occurs in the free association model. The polymerization temperature $T_p$ determined from the maximum of $C_V(T)$ departs significantly from the ideal polymerization temperature $T_p^{(o)}$ predicted by the Dainton–Ivin equation,[33]

$$T_p^{(o)} = \frac{\Delta h_p}{\Delta s_p + k_B \ln \phi_1^o}, \tag{24}$$

which is often assumed to describe associating systems generally.[34] Large deviations of $T_p$ from $T_p^{(o)}$ for other polymerization models are discussed in Sec. V.

Other basic properties of associating polymer solutions are the extent of polymerization $\Phi$ and the average chain length $L \equiv \langle i \rangle$. The former quantity $\Phi$ is defined as the fraction of monomers converted into polymers,

$$\Phi \equiv \frac{\phi_1^o - \phi_1}{\phi_1^o} = \frac{1}{\phi_1^o}\frac{CA^2(2-A)}{(1-A)^2}. \tag{25}$$

The variation of $\Phi$ with $T$ at a given $\phi_1^o$ is always monotonic because the sign of the derivative,

$$\left.\frac{\partial \Phi}{\partial T}\right|_{\phi_1^o} = \left[\frac{1}{\phi_1^o T}\frac{2CA^2\phi_1}{(1-A)^3\phi_1^o + 2CA^2}\right]\frac{\Delta h_p}{k_B T}, \quad 0<A<1, \quad C>0,$$

is dictated by a sign of the "sticking energy" $\Delta h_p$. The extent of polymerization increases with $T$ when $\Delta h_p > 0$ (polymerization upon heating) and decreases monotonically with $T$ when $\Delta h_p < 0$ (polymerization upon cooling). The average chain length $L$ is determined from an average over *all* monomer containing species in the system

$$L \equiv \frac{\Sigma_{i=1}^{\infty} \phi_i}{\Sigma_{i=1}^{\infty} \frac{\phi_i}{i}} = \frac{\phi_1^o}{\phi_1^o - \frac{CA^2}{(1-A)^2}}. \tag{26}$$

Equations (25) and (26) imply that the average chain length $L$ and the extent of polymerization $\Phi$ are related to each other as,

$$L = \frac{2-A}{2-A-\Phi}. \tag{27}$$

The variation of $L(T)$ for a given $\phi_1^o$ is likewise monotonic since the sign of the derivative $\partial L/\partial T$ is also controlled by the sign of $\Delta h_p$. For polymerization upon cooling, the average chain length $L$ in the low temperature regime ($T \ll T_p$) exhibits the well-known scaling[23–25] $L \sim (\phi_1^o)^{1/2} \times \exp[-\Delta h_p/(2k_BT)]$ (see the Appendix), so that $L$ only diverges in this model as $T \to 0^+$. While many properties that characterize the polymerization transition of associating solutions, such as those defined by Eqs. (21)–(23) and (25)–(26), are independent of the Flory–Huggins interaction parameter $\chi$, other thermodynamic quantities, such as the osmotic pressure, second virial coefficient, theta temperature, and critical temperature and critical composition (for phase separation), are strongly influenced by both $\chi$ and the free energy parameters $\Delta h_p$ and $\Delta s_p$. We now summarize the essential thermodynamic relations for some of these properties.

The osmotic pressure $\Pi$ can be evaluated from the Helmholtz free energy $F$ as

$$\begin{aligned} \frac{\Pi a^3}{k_BT} &= -\frac{a^3}{k_BT}\left.\frac{\partial F}{\partial V}\right|_{T,n_1^o} \\ &= -\frac{1}{k_BT}\left.\frac{\partial F}{\partial n_s}\right|_{T,n_1^o} \\ &= -\ln(1-\phi_1^o) - (\phi_1^o)^2\chi - \frac{CA^2}{(1-A)^2}, \end{aligned} \tag{28}$$

with $a^3 = V/N_l$ being the volume associated with a single lattice site. Expanding the logarithmic term of the right-hand side of Eq. (28) around $\phi_1^o \to 0$ and rearranging the ratio $CA^2/(1-A)^2$ into a series expansion in $\phi_1^o$ yield the osmotic virial expansion,

$$\frac{\Pi a^3}{k_BT} = \phi_1^o + (\phi_1^o)^2 A_2 + (\phi_1^o)^3 A_3 + \cdots, \tag{29}$$

where the second ($A_2$) and third ($A_3$) virial coefficients are identified as

$$A_2 = (1/2) - \chi(T) - C(T)G(T)^2, \tag{30}$$

and

$$A_3 = (1/3) + 2C(T)G(T)^3[2C(T)G(T) - 1], \tag{31}$$

with the notation $C(T)$ used for $C$ of Eqs. (17) and (18) to emphasize its temperature dependence. The factors $G(T)$ are defined as

$$G \equiv (z-1)K_p \quad \text{(fully flexible chains)},$$

and

$$G \equiv K_p \quad \text{(stiff chains)}.$$

The products $C(T)G(T)$ in Eqs. (30)–(31) represent the effective contributions to the virial coefficients which arise from association. The theta temperature is defined as the temperature at which $A_2$ vanishes identically and may be obtained numerically from Eq. (30).

Equations (19) and (20) indicate that the free association model formally contains only one independent composition variable ($\phi_1^o$), which implies that the stability condition for the existence of a stable homogeneous phase is simply

$$\left.\frac{\partial^2 F/(N_l k_B T)}{\partial \phi_1^{o^2}}\right|_{N_l,T} > 0.$$

Calculating the second derivative of $F$ with respect to $\phi_1^o$ and equating it to zero produce the constant volume spinodal curves $T = T(\phi_1^o)$ as the solution of

$$\frac{1}{\phi_1^o + \frac{2CA^2}{(1-A)^3}} + \frac{1}{1-\phi_1^o} - 2\chi = 0, \tag{32}$$

where the quantity $A = A(\phi_1^o, T)$ or, equivalently, the compositon $\phi_1 = A/G$ of unreacted monomers is determined numerically from the mass conservation condition in Eq. (19).

A maximum (or minimum) of the spinodal curve defines the critical temperature $T_c$ and critical composition $\phi_c \equiv (\phi_1^o)_c$. Knowledge of the critical parameters $T_c$ and $\phi_c$ in conjunction with Eq. (28) enables calculating the critical osmotic compressibility factor $Z_c = \Pi_c a^3/(k_BT_c\phi_c)$, another important thermodynamic quantity for associating systems.

The spinodal condition in Eq. (32) can be transformed to the following form:

$$\frac{1}{\phi_1^o\left[1 + \frac{2(1-1/L)}{1-A}\right]} + \frac{1}{1-\phi_1^o} - 2\chi = 0, \tag{33}$$

which evidently resembles the spinodal condition for polymer solutions. In the absence of polymerization ($L = 1$, $A = 0$), Eq. (33) coincides with the spinodal equation for the monomer–solvent system. Since $(1-A)$ is positive for all compositions $\phi_1^o$ and temperatures $T$, the coefficient that multiplies $\phi_1^o$ in Eq. (33) is also positive, and, consequently, both $T_c$ and $\phi_c$ of the free association system are well defined as long as the exchange energy $\epsilon_{\mathrm{FH}}$ (reflecting the net short range, isotropic interaction between the associating species and solvent) is positive. A more precise analysis (see the Appendix) demonstrates that the critical composition $\phi_c$ scales with $\epsilon_{\mathrm{FH}}$ in the low temperature regime ($T_c \ll T_p$) as

$$\phi_c \sim \left[\frac{1}{\exp[-\Delta f_p/(2k_B\epsilon_{\mathrm{FH}})]}\right]^{1/5},$$

$$\Delta h_p < 0, \quad \Delta s_p < 0, \quad T_c \ll T_p.$$

The above scaling, when reexpressed in terms of the average degree of polymerization $L$,

$$\phi_c \sim L^{-2/5}, \quad \Delta h_p < 0, \quad \Delta s_p < 0, \quad T_c \ll T_p, \tag{34}$$

exhibits a departure from well-known prediction of FH theory[27] for monodisperse polymer solutions, $\phi_c \sim N^{-1/2}$,

with $N$ denoting the polymerization index. The scaling in Eq. (34), however, is close to the observed scaling between $\phi_c$ and chain length in real polymer solutions, where an exponent near $-0.4$ is found.[35] The critical temperature $T_c$ is positive for any positive $\epsilon_{\mathrm{FH}}$ and smoothly approaches zero as $\epsilon_{\mathrm{FH}} \to 0$,

$$T_c \simeq 2\epsilon_{\mathrm{FH}}, \quad \Delta h_p < 0, \ \Delta s_p < 0, \quad T_c \ll T_p, \tag{35}$$

coinciding, of course, with the critical temperature of polymer solutions in the limit of infinite molecular weight polymers.[27]

## III. ACTIVATED EQUILIBRIUM POLYMERIZATION

Many physical systems undergo secondary kinetic processes that serve to regulate the dynamic clustering process. For example, the polymerization of sulfur begins with the activation step involving the opening of the $S_8$ ring, a necessary kinetic event that ''activates'' the monomer species for subsequent polymerization.[25] The propagation of monomeric G-actin to F-actin filaments is believed to require conformational transitions in the G-actin monomer to activate the monomer for further association.[36] Simulations of ionic fluids[31] suggest that ion-pairing occurs as a prelude to subsequent clustering of dipolar and quadrupolar species into linear and branched polymer species. The activated equilibrium polymerization corresponds to case II in the classification scheme[10] of Tobolsky and Eisenberg. We generalize this former treatment by introducing chain stiffness and solvent quality effects into a systematic description of all thermodynamic properties, including the coupling between phase separation and clustering.

The simplest model of activated polymerization emerges from considering the minimal reaction scheme,[10]

$$M_1 \rightleftharpoons M_1^*, \tag{36}$$

$$M_1^* + M_1 \rightleftharpoons M_2, \tag{37}$$

$$M_i + M_1 \rightleftharpoons M_{i+1}, \quad i = 2,3,\ldots,\infty, \tag{38}$$

in which the activated species $M_1^*$ reacts only with nonactivated monomers $M_1$ to form dimers. Alternatively, only activated monomers and polymers can participate in the chain propagation processes,

$$M_1 \rightleftharpoons M_1^*, \tag{39}$$

$$M_1^* + M_1^* \rightleftharpoons M_2, \tag{40}$$

$$M_i + M_1^* \rightleftharpoons M_{i+1}, \quad i = 2,3,\ldots,\infty. \tag{41}$$

The description of equilibrium polymerization in Eqs. (39)–(41) is mathematically isomorphic to that corresponding to Eqs. (36)–(38) because both models become identical upon introducing an appropriate redefinition of the corresponding free energy parameters as discussed in the following. Moreover, the free association model is evidently a limit of Eqs. (39)–(41) where the activation process in Eq. (39) is assumed to proceed to completion.

The reaction scheme in Eqs. (36)–(38) is further specified by designating $\Delta f_a = \Delta h_a - T\Delta s_a$ and $\Delta f_p = \Delta h_p - T\Delta s_p$ as the free energies of activation and polymerization, respectively, and by taking, for simplicity, both the enthalpies $\Delta h_p$ and entropies $\Delta s_p$ associated with dimer formation [Eq. (37)] and with the propagation process [Eq. (38)] as identical. The Helmholtz free energy $F$ of the equilibrium system (consisting of nonactivated monomers, activated monomers, and polymers) is given by

$$\frac{F}{N_l k_B T} = \phi_s \ln \phi_s + \phi_1^* \ln \phi_1^* + \sum_{i=1}^{\infty} \frac{\phi_i}{i} \ln \phi_i + \phi_s \phi_1^* \chi + \phi_s \chi \sum_{i=1}^{\infty} \phi_i + \phi_1 f_1^* + \sum_{i=2}^{\infty} \phi_i f_i. \tag{42}$$

Equation (42) differs from Eq. (4) for the free association model by the appearance of the terms associated with the presence of the activated monomers whose volume fraction and dimensionless specific free energy are denoted by $\phi_1^*$ and $f_1^*$, respectively. For simplicity, short range van der Waals interactions are represented in Eq. (42) [as in Eq. (4)] by a single interaction parameter $\chi$ that describes the average effective interactions between the solvent and monomers (including activated ones) of the associating species $M$.

The specific free energies $\{f_i\}$ emerge from the FH theory[27] as

$$f_1 = 0, \quad f_1^* = \frac{\Delta f_a}{k_B T}, \tag{43}$$

$$f_2 = \frac{1}{2}\ln\left[\frac{2}{z\ 2}\right] + 1 - \frac{1}{2} + \frac{1}{2}\Delta f_p + \frac{1}{2}\frac{\Delta f_a}{k_B T} \quad \text{(fully flexible chains)}, \tag{44}$$

$$f_i = \frac{1}{i}\ln\left[\frac{2(z-1)^2}{z\ i}\right] + \frac{i-1}{i} - \ln(z-1) + \frac{i-1}{i}\frac{\Delta f_p}{k_B T} + \frac{1}{i}\frac{\Delta f_a}{k_B T}, \quad i \geqslant 3 \quad \text{(fully flexible chains)}, \tag{45}$$

and

$$f_i = \frac{1}{i}\ln\left[\frac{2}{z\ i}\right] + 1 - \frac{1}{i} + \frac{i-1}{i}\frac{\Delta f_p}{k_B T} + \frac{1}{i}\frac{\Delta f_a}{k_B T}, \quad i \geqslant 2 \quad \text{(stiff chains)}, \tag{46}$$

while the chemical potentials $\{\mu_i\}$ of the individual species can be evaluated from the free energy in Eq. (42). Applying the equilibrium conditions [see Eq. (7)] appropriate for the reactions in Eqs. (36)–(38) yields the distribution of volume fractions $\{\phi_i\}$,

$$\phi_1^* = \phi_1 K_a, \quad K_a = \exp(-\Delta f_a / k_B T)$$

and

$$\phi_i = iCA^i, \quad i \geqslant 2. \tag{47}$$

The quantities $A$ and $C$ are given by

$$A \equiv \phi_1 (z-1) K_p \quad \text{(fully flexible chains)}, \tag{48}$$

$$A \equiv \phi_1 K_p \quad \text{(stiff chains)}, \tag{49}$$

and

$$C \equiv \frac{z}{2(z-1)^2}\frac{K_a}{K_p} \quad \text{(fully flexible chains)}, \tag{50}$$

$$C \equiv \frac{z}{2}\frac{K_a}{K_p} \quad \text{(stiff chains)}. \tag{51}$$

where $K_a = \exp(-\Delta f_a/k_BT)$ denotes the equilibrium constant for monomer activation [see Eq. (36)] and $K_p = \exp(-\Delta f_p/k_BT)$ designates the equilibrium constant for polymerization [see Eqs. (37) and (38)] in the stiff chain system. [The earlier assumption of identical free energy parameters for dimerization—Eq. (37)—and chain propagation—Eq. (38)—implies an identical $K_p$ for these two processes.] The equilibrium constant of reactions (37) and (38) in the fully flexible chain system is defined as the product of $K_p$ and $(z-1)$.

The existence of equilibrium conditions analogous to those characterizing the free association model implies the validity of an alternative polymerization mechanism in which chains can also form (or break) through chain coupling (or scission). Hence, Eq. (38) may be generalized to the reaction scheme,

$$M_j + M_k \rightleftharpoons M_{j+k}, \quad j = 2,3,\ldots,\infty, \quad k = 1,2,\ldots,\infty.$$

Notice that Eq. (47) has the identical form as Eq. (14). Moreover, Eqs. (48)–(51) reduce to the free association model Eqs. (15)–(18) when $\Delta f_a = 0$ (i.e., $K_a = 1$), as they must. This formal identity does not imply, however, that $A$ and $\{\phi_i\}$ have the same values for these two models since the mass conservation constraint for the activated association model,

$$\phi_1^o = \phi_1[1 + K_a] + \frac{CA^2(2-A)}{(1-A)^2}, \tag{52}$$

contains the extra term $\phi_1^* = \phi_1 K_a$ that is absent in Eq. (19). Additional differences arise, of course, from the various definitions of the prefactor $C$ [compare Eqs. (50) and (51) with Eqs. (17) and (18)]. Surprisingly, the Helmholtz free energy of Eq. (42) reduces [after inserting Eq. (47) and performing the summations] to the simple form

$$\frac{F}{N_l k_B T} = (1-\phi_1^o)\ln(1-\phi_1^o) + \phi_1^o \ln \phi_1 + (1-\phi_1^o)\phi_1^o \chi + \frac{CA^2}{(1-A)^2}, \tag{53}$$

which does not explicitly contain the volume fraction $\phi_1^*$. Equation (53) is *formally identical* to Eq. (20).

The internal energy $U$, specific heat $C_V$, and entropy $S$ of the system are represented, however, by more lengthy formulas than the corresponding Eqs. (21)–(23),

$$\frac{U}{N_l k_B T} = \frac{1}{N_l k_B T}\left.\frac{\partial[F/(k_BT)]}{\partial[1/k_BT]}\right|_{N_l} = (1-\phi_1^o)\phi_1^o \chi + \frac{CA^2}{(1-A)^2}\left(\frac{\Delta h_p}{k_BT} - \frac{\Delta h_a}{k_BT}\right) + (\phi_1^o - \phi_1)\frac{\Delta h_a}{k_BT}, \tag{54}$$

$$\frac{S}{N_l k_B} = \frac{U}{N_l k_B T} - \frac{F}{N_l k_B T} = -(1-\phi_1^o)\ln(1-\phi_1^o) - \phi_1^o \ln \phi_1 + \frac{CA^2}{(1-A)^2}\left[\frac{\Delta h_p}{k_BT} - \frac{\Delta h_a}{k_BT} - 1\right] + (\phi_1^o - \phi_1)\frac{\Delta h_a}{k_BT}, \tag{55}$$

and

$$\frac{C_V}{N_l k_B} = \frac{1}{N_l k_B}\left.\frac{\partial U}{\partial T}\right|_{N_l} = \left(\frac{\Delta h_p}{k_BT} - \frac{\Delta h_a}{k_BT}\right)^2 \frac{2CA^2}{(1-A)^3}\left[\frac{\phi_1^o}{\phi_1^o + \frac{2CA^2}{(1-A)^3}} - \frac{1-A}{2}\right] + \left(\frac{\Delta h_a}{k_BT}\right)^2 \frac{\phi_1}{\phi_1^o + \frac{2CA^2}{(1-A)^3}} \times \left[\phi_1^o - \phi_1 + \frac{2CA^2}{(1-A)^3}\right] + 2\left(\frac{\Delta h_p}{k_BT} - \frac{\Delta h_a}{k_BT}\right)\left(\frac{\Delta h_a}{k_BT}\right) \times \frac{\phi_1}{\phi_1^o + \frac{2CA^2}{(1-A)^3}}\frac{2CA^2}{(1-A)^3}. \tag{56}$$

Setting $\Delta h_a = 0$ in Eqs. (54)–(56) recovers the free association model Eqs. (21)–(23), as it must.

The definitions of the extent of polymerization $\Phi$ and the average degree of polymerization $L$ must explicitly include the presence of activated monomers,

$$\Phi \equiv \frac{\phi_1^o - \phi_1 - \phi_1^*}{\phi_1^o} = \frac{1}{\phi_1^o}\frac{CA^2(2-A)}{(1-A)^2}, \tag{57}$$

and

$$L \equiv \frac{\phi_1^* + \Sigma_{i=1}^{\infty}\phi_i}{\phi_1^* + \Sigma_{i=1}^{\infty}\frac{\phi_i}{i}} = \frac{\phi_1^o}{\phi_1^o - \frac{CA^2}{(1-A)^2}}. \tag{58}$$

Since the right-hand sides of Eqs. (57) and (58) are the same as those in Eqs. (25) and (26), Eq. (27),

$$L = \frac{2-A}{2-A-\Phi},$$

still applies. In contrast to the free association model, Eqs. (57) and (58) indicate that both the extent polymerization $\Phi$ and the average chain length $L$ are no longer generally monotonic functions of temperature when an activated process is present. For instance, the temperature derivative of $\Phi$,

$$\left.\frac{\partial\Phi}{\partial T}\right|_{\phi_1^o}=\frac{1}{\phi_1^o T\left(\phi_1^o+\dfrac{2CA^2}{(1-A)^3}\right)}\left[\frac{\Delta h_p}{k_BT}\frac{2CA^2\phi_1}{(1-A)^3}+\frac{\Delta h_a}{k_BT}\frac{CA^2(2-A)\phi_1}{(1-A)^2}+\left(\frac{\Delta h_p}{k_BT}-\frac{\Delta h_a}{k_BT}\right)\frac{2CA^2\phi_1^*}{(1-A)^3}\right],$$

$$0<A<1,\quad C>0, \tag{59}$$

may vanish when $\Delta h_p$ and $\Delta h_a$ have different or the same signs. In the latter case, $(\partial\Phi/\partial T)|_{\phi_1^o}=0$ only if $|\Delta h_a|>|\Delta h_p|$.

The identical form of the free energy $F$ for the free association and activated association models implies a common expression for the osmotic pressure [see Eq. (28)],

$$\frac{\Pi a^3}{k_BT}=-\ln(1-\phi_1^o)-(\phi_1^o)^2\chi-\frac{CA^2}{(1-A)^2},$$

and for the spinodal stability condition [see Eqs. (32) and (33)],

$$\frac{1}{\phi_1^o+\dfrac{2CA^2}{(1-A)^3}}+\frac{1}{1-\phi_1^o}-2\chi=0,$$

or

$$\frac{1}{\phi_1^o\left[1+\dfrac{2(1-1/L)}{1-A}\right]}+\frac{1}{1-\phi_1^o}-2\chi=0.$$

As already mentioned, this commonality does not lead to the same values of $\Pi$, $T_c$, $\phi_c$, etc., in these two models due to the different mass conservation equations determining $A$. The second and the third virial coefficients are given by different expressions than those in Eqs. (30) and (31) for the free association model,

$$A_2=\frac{1}{2}-\chi-\frac{CG_p^2}{(1+K_a)^2}, \tag{60}$$

and

$$A_3=\frac{1}{3}+\frac{2CG_p^3}{(1+K_a)^3}\left[\frac{2CG_p}{1+K_a}-1\right], \tag{61}$$

where $G_p=\alpha K_p$ and $\alpha$ equals to $(z-1)$ and 1 for fully flexible and stiff chains, respectively. The validity of Eqs. (32) and (33) also suggests that the critical point for the activated association solutions always exists if $\epsilon_{\mathrm{FH}}$ is positive. On the other hand, the asymptotic analysis of the critical properties (see the Appendix) is no longer analytically tractable because of the presence of an additional parameter (i.e., the free energy of activation $\Delta f_a$). We can distinguish, however, two limiting behaviors of $\phi_c$ and $T_c$ for activated association systems. Consider polymerization upon cooling (i.e., $\Delta h_p<0$, $\Delta s_p<0$) in the low temperature regime ($T_c\ll T_P$) and assume, for simplicity, that the entropies of activation and polymerization are identical (i.e., $\Delta s_a=\Delta s_p$). The first limiting case emerges when $\Delta h_a\geqslant 0$. Then, we obtain $A\to 1$, $L\gg 1$, $\phi_c\to 0$, and $\lim_{\epsilon_{\mathrm{FH}}\to 0}T_c\simeq 2\epsilon_{\mathrm{FH}}\to 0$, in analogy to the free association system (and polymer solutions). Another limiting case arises when $|\Delta h_a|\geqslant|\Delta h_p|$, which, in turn, implies $A\to 0$, $L\to 1$, $\phi_c\to 1/2$ and $\lim_{\epsilon_{\mathrm{FH}}\to 0}T_c=(1/2)\epsilon_{\mathrm{FH}}\to 0$, resembling a monomer–solvent system. Other choices of $\Delta h_a$ (i.e., $0<|\Delta h_a|<|\Delta h_p|$) yield the critical composition $\phi_c$ between 1/2 and 0 and the critical temperature $T_c$ between $(1/2)\epsilon_{\mathrm{FH}}$ and $2\epsilon_{\mathrm{FH}}$.[37]

For completeness, expressions for $A$ and $C$ are quoted in the following for the activated association model in which only the activated monomers and polymers can participate in the chain propagation [see Eqs. (39)–(41)],

$$A'\equiv\phi_1'(z-1)K_p'K_a'\quad\text{(fully flexible chains)},$$

$$A'\equiv\phi_1'K_p'K_a'\quad\text{(stiff chains)},$$

and

$$C'\equiv\frac{z}{2(z-1)^2}\frac{1}{K_p'}\quad\text{(fully flexible chains)},$$

$$C'\equiv\frac{z}{2}\frac{1}{K_p'}\quad\text{(stiff chains)}.$$

The superscript prime is used to distinguish variables from the corresponding quantities of the alternative activated association model described by Eqs. (36)–(38). Both models predict identical properties upon redefinition of the free energy parameters,

$$\Delta f_a'=\Delta f_a,\quad K_a'\equiv\exp[-(\Delta f_a'/k_BT)]=K_a, \tag{62}$$

and

$$\Delta f_p'=\Delta f_p-\Delta f_a,\quad K_p'\equiv\exp[-\Delta f_p'/k_BT]=K_p/K_a. \tag{63}$$

While the analysis in this section is performed assuming equal volumes for solvent molecules and for monomers of the associating species, our recent treatement[38] of actin polymerization shows that all equations for the basic thermodynamic properties are unchaged when the volume ratio $v=v_m/v_s$ differs from unity, because the parameter $v$ can be absorbed into the definition of $\Delta s_p$. This formal insensitivity of the basic equations to $v$ is also maintained for the other association models.

## IV. LIVING POLYMERIZATION

In contrast to the free and activated association models, chain growth in the living polymerization system is induced by a chemical ''initiator'' $I$. This type of polymerization corresponds to case I in the classification scheme of Tobolsky and Eisenberg[10] and has been discussed extensively in our previous papers.[1–3] The equilibrium polymerization of poly($\alpha$-methylstyrene) in methylcyclohexane with sodium naphthalide as an initiator provides a specific example of a system exhibiting this type of dynamic clustering transition.[4,5] Here we briefly review some essential characteristics of this model and include a description of new properties for completeness and comparison with the other two models of association.

One possible mechanism for the initiation process involves a bifunctional dimer $M_2I_2$ as the smallest propagating species and postulates that it is formed by an irreversible reaction,

$$2M_1+2I\rightarrow M_2I_2. \tag{64}$$

Polymerization proceeds by the successive addition of monomers $M_1$ to dimers $M_2I_2$, trimers $M_3I_2$, etc., which, according to the chemical equlibrium, can sequentially disintegrate as well,

$$M_iI_2+M_1\rightleftharpoons M_{i+1}I_2, \quad i=2,3,\ldots,\infty. \tag{65}$$

The Helmholtz free energy $F$ of the system is given by

$$\frac{F}{N_lk_BT}=\phi_s\ln\phi_s+\phi_1\ln\phi_1+\sum_{i=2}^{\infty}\frac{\phi_i}{i+2}\ln\phi_i+\phi_s\phi_1\chi + \phi_s\chi\sum_{i=2}^{\infty}\phi_i+\sum_{i=2}^{\infty}\phi_if_i, \tag{66}$$

where $\phi_1$, $\phi_s=1-\phi_1^o-\phi_I$, and $\{\phi_i\}$ denote the volume fractions for the residual (i.e., unpolymerized) monomers, the solvent, and polymers, respectively, and $\phi_I$ is the initial composition of initiator. The equilibrium system does not contain free initiator molecules because of the assumed irreversibility of the initiation reaction in Eq. (64). Again, for simplicity, we assume that different types of monomers (i.e., unpolymerized or belonging to polymers) interact with solvent with the same van der Waals energies and display no preference in the mutual interactions, i.e., $\chi_{mm'}=0$. Consequently, there is only a single interaction parameter $\chi=\epsilon_{\mathrm{FH}}/T$ in Eq. (66). The dimensionless specific free energies $\{f_i\}$ of $i$-mers are obtained within FH theory as

$$f_i=\frac{1}{i+2}\ln\left[\frac{2(z-1)^2}{z(i+2)}\right]+\frac{i+1}{i+2}-\ln(z-1) + \frac{i-1}{i+2}\frac{\Delta f_p}{k_BT}, \quad i\geqslant 2 \quad \text{(fully flexible chains)}, \tag{67}$$

and

$$f_i=\frac{1}{i+2}\ln\left[\frac{2}{z(i+2)}\right]+\frac{i+1}{i+2}-\frac{i}{i+2}+\frac{i-1}{i+2}\frac{\Delta f_p}{k_BT}, \quad i\geqslant 2 \quad \text{(stiff chains)}. \tag{68}$$

The condition of chemical equilibrium imposes the relation between the chemical potentials $\{\mu_i\}$, $\mu_2$, and $\mu_1$ of $i$-mers $M_iI_2$ ($i\geqslant 3$), dimers $M_2I_2$, and monomers $M_1$, respectively,

$$\mu_i=\mu_2+(i-2)\mu_1, \quad i=3,4,\ldots,\infty, \tag{69}$$

which, in turn, can be converted to mass action form,

$$\ln\left[\frac{\phi_i}{\phi_2\phi_m^{i-2}}\right]=i-2-(i+2)f_i+4f_2, \quad i=3,4,\ldots,\infty. \tag{70}$$

The relation in Eq. (69) *cannot* be rearranged to a form admitting of alternative mechanisms of chain propagation that involve chain coupling and scission.

Combining Eqs. (67)–(68) and (70) leads to the equilibrium distribution of volume fractions $\{\phi_i\}$,

$$\phi_i=(i+2)CA^{i-2}, \quad i\geqslant 2, \tag{71}$$

where the quantities $A$ and $C$ are defined as

$$A\equiv\phi_1(z-1)K_p \quad \text{(fully flexible chains)}, \tag{72}$$

$$A\equiv\phi_1K_p, \quad K_p=\exp[-\Delta f_p/k_BT] \quad \text{(stiff chains)}, \tag{73}$$

and

$$C\equiv(1/4)\phi_2=(1/2)\phi_I(1-A). \tag{74}$$

The initiator composition $\phi_I$ and the intial monomer composition $\phi_1^o$ are related through the mass conservation condition,

$$\phi_1^o=\phi_1+\frac{\phi_I}{2}\frac{(2-A)}{(1-A)}. \tag{75}$$

Equation (75) can be solved analytically for $\phi_1$, producing

$$\phi_1=\frac{B-\sqrt{B^2-4(\phi_1^0-\phi_I)G}}{2G}, \tag{76}$$

where the notation

$$B\equiv 1+[\phi_1^0-(1/2)\phi_I]G, \quad G\equiv\alpha K_p, \tag{77}$$

is employed with the coefficient $\alpha$ equal to $(z-1)$ or 1 for fully flexible or stiff chains, respectively. After inserting Eq. (71) and performing the summations in Eq. (66), the Helmholtz free energy $F$ for the equilibrium system reduces to the following form:

$$\frac{F}{N_lk_BT}=(1-\phi_1^o-\phi_I)\ln(1-\phi_1^o-\phi_I)+(\phi_1^o-\phi_I)\ln\phi_1 + \phi_1^o-\phi_1+(\phi_1^o+\phi_I)(1-\phi_1^o-\phi_I)\chi + \frac{\phi_I}{2}\left[\ln\left(\frac{\phi_I(1-A)\alpha^2}{z}\right)+\frac{\Delta f_p}{k_BT}+1\right], \tag{78}$$

which is equivalent to the more complicated Eq. (3) of Paper II. The extent of polymerization $\Phi$ and the average chain length $L$ can be expressed in terms of the quantity $A$ and the dimensionless initiator concentration $r=\phi_I/\phi_1^o$ as

$$\Phi\equiv\frac{\phi_1^o-\phi_1}{\phi_1^o}=\frac{r}{2}\frac{(2-A)}{(1-A)}, \tag{79}$$

and

$$L\equiv\frac{\phi_1+\Sigma_{i=2}^{\infty}\phi_i\frac{i}{i+2}}{\phi_1+\Sigma_{i=2}^{\infty}\frac{\phi_i}{i+2}}=\frac{\phi_1^0(1-A)}{(1-A)\phi_1^o-(1/2)\phi_I}, \tag{80}$$

while other thermodynamic quanties of the system (such as the internal energy $U$, entropy $S$, or specific heat $C_V$) follow directly from Eq. (78),

$$\frac{U}{N_l k_B T}=\frac{1}{N_l k_B T}\frac{\partial[F/(k_B T)]}{\partial[1/k_B T]}$$
$$=(1-\phi_1^o-\phi_I)(\phi_1^o+\phi_I)\chi+\left[\phi_1^o-\phi_1-\frac{\phi_I}{2}\right]\frac{\Delta h}{k_B T}, \tag{81}$$

$$\frac{S}{N_l k_B}=\frac{U-F}{N_l k_B T}=-(1-\phi_1^o-\phi_I)\ln(1-\phi_1^o-\phi_I)$$
$$-(\phi_1^o-\phi_I)\ln\phi_1+\left[\phi_1^o-\phi_1-\frac{\phi_I}{2}\right]$$
$$\times\left[\frac{\Delta h_p}{k_B T}-1\right]-\frac{\phi_I}{2}\left[\ln\left(\frac{\phi_I(1-A)\alpha^2}{z}\right)\right.$$
$$\left.+\frac{\Delta f_p}{k_B T}+2\right], \tag{82}$$

and

$$\frac{C_V}{N_l k_B}=\frac{1}{N_l k_B}\frac{\partial U}{\partial T}\bigg|_{N_l}=\left(\frac{\Delta h}{k_B T}\right)^2\frac{(\phi_1^o-\phi_1-\phi_I)\phi_1}{\phi_1^o-\phi_1 A-\phi_I}. \tag{83}$$

Equation (83) can be transformed even to a more compact form involving the temperature derivative of the extent of polymerization $\Phi$,

$$\frac{C_V}{N_l k_B}=\phi_1^o\frac{\Delta h_p}{k_B}\frac{\partial\Phi}{\partial T}\bigg|_{\phi_1^o}, \tag{84}$$

which clearly demonstrates that the temperature $T_p$ at which $C_V(T)$ has a maximum coincides with the temperature $T_\Phi$ at which the extent of polymerization $\Phi$ exhibits an inflection point (as a function of $T$).[22] The temperature $T_p$ and $T_\Phi$ no longer are identical for the free and activated association systems because the specific heat $C_V$ for these models depends on the derivative $\partial\Phi/\partial T$ in a more complicated fashion. For instance, the specific heat in the free association model is given by

$$\frac{C_V}{N_l k_B}=\phi_1^o\frac{\Delta h_p}{k_B}\left[\frac{\partial\Phi}{\partial T}\bigg|_{\phi_1^o}(1-\Phi)-\frac{\Delta h_p}{k_B T^2\phi_1^o}\frac{CA^2}{(1-A)^2}\right].$$

Not only are $T_p$ and $T_\Phi$ equal for the living polymerization system, but both these temperatures approach the ideal polymerization temperature $T_p^{(o)}$ of the Dainton–Ivin equation in the $r\to 0$ limit. As noted previously by Kennedy and Wheeler,[22] the magnitude of the peak $C_V^*(r\to 0^+)$ in $C_V(r\to 0^+)$ depends only on $\Delta h_p$ and $T_p^{(o)}$,

$$\frac{C_V^*(r\to 0^+)}{N_l k_B}=\left[\frac{\Delta h_p}{k_B T_p^{(o)}}\right]^2.$$

The specific heat maximum $C_V^*(r\to 0^+)$ is actually insensitive to $\Delta h_p$, since $T_p^{(o)}\sim\Delta h_p$. Specifically, Eq. (24) implies,

$$\frac{C_V^*(r\to 0^+)}{N_l k_B}=\left[\frac{\Delta s_p}{k_B}+\ln\phi_1^o\right]^2,$$

indicating that only the sum of the entropies of mixing and polymerization determines the magnitude of $C_V^*$. The logarithmic term characteristically predominates at low $\phi_1^o$, and therefore $C_V^*$ of associating solutions tends to increase with their dilution.[1] This concentration dependence of $C_V^*$ is apparently a singular feature of equilibrium polymerization and can be used to discriminate this kind of particle association from phase separation.[39]

The living polymerization solution is formally a three component system characterized by two independent composition variables $\phi_1^o$ and $\phi_I$. Consequently, the constant volume spinodal condition,[40]

$$D\equiv\frac{\partial^2 F}{\partial\phi_1^{o2}}\bigg|_{N_l,T,\phi_I}\frac{\partial^2 F}{\partial\phi_I^2}\bigg|_{N_l,T,\phi_1^o}-\left[\frac{\partial^2 F}{\partial\phi_1^o\partial\phi_I}\bigg|_{N_l,T}\right]^2=0, \tag{85}$$

involves three types of second-order composition derivatives of the Helmholtz free energy $F$. After some algebra, Eq. (85) can be converted to the compact form

$$\frac{1}{1-\phi_1^o-\phi_I}+\frac{1}{\dfrac{\phi_1}{\dfrac{\partial\phi_1}{\partial\phi_1^o}\Big|_{N_l,T}}+\dfrac{2(\phi_1^o+\phi_I-\phi_1)^2}{\phi_I}}-2\chi=0, \tag{86}$$

where the derivative $\partial\phi_1/\partial\phi_1^o$ in Eq. (85) can be obtained from Eq. (76). Equation (86) resembles the spinodal condition for the free and activation association systems which both undergo phase separation (with well-defined critical composition and critical temperature for any positive $\epsilon_{FH}$). This apparent resemblance of the spinodal conditions is not, however, sufficient to prove that the critical point also always exists for the living polymerization solution when $\epsilon_{FH}>0$. Generally, the spinodal $T=T(\phi_1^o,\phi_I)$ obtained from Eq. (86) is a surface, but often it is convenient to consider its projection onto a line $T=T(\phi_1^o)$ for $r=\phi_I/\phi_1^o$ fixed. (Experiments are indeed often performed for systems with a constant initiator fraction $r$.[4,5,34]) Under this assumption, the critical point for the living polymerization system is determined by the vanishing of the derivative $(\partial D/\partial\phi_1^o)|_{N_l,T,\phi_I}$, where $D$ is defined in Eq. (85). The constraint,

$$\frac{\partial D}{\partial\phi_1^o}\bigg|_{N_l,T,\phi_I}=0,$$

is equivalent to the vanishing of the combination of the third derivatives of $F$,

$$\frac{\partial^3 F}{\partial\phi_1^{o3}}\bigg|_{N_l,T,\phi_I}+\frac{\partial^3 F}{\partial\phi_1^o\partial\phi_I^2}\bigg|_{N_l,T}\left(\frac{d_{12}}{d_{22}}\right)^2$$
$$-2\frac{\partial^3 F}{\partial\phi_1^{o2}\partial\phi_I}\bigg|_{N_l,T}\left(\frac{d_{12}}{d_{22}}\right)=0 \tag{87}$$

with

$$d_{12}\equiv\frac{\partial^2 F}{\partial\phi_1^o\partial\phi_I}\bigg|_{N_l,T},\quad d_{22}\equiv\frac{\partial^2 F}{\partial\phi_I^2}\bigg|_{N_l,T,\phi_1^o}.$$

An asymptotic analysis of Eqs. (87) and (86) is specialized to the case of polymerization upon cooling ($\Delta h_p<0$, $\Delta s_p<0$) and to the low temperature regime ($T_c\ll T_p$) where $G\gg 1$.

The critical composition $\phi_c$ is found to be determined exclusively by the ratio $r=\phi_I/\phi_1^o$ of the initatior composition $\phi_I$ and the initial monomer concentration $\phi_1^o$,

$$\phi_c=\sqrt{\frac{r}{2}}\left[1-\sqrt{\frac{r}{2}}+O\left(\frac{r}{2}\right)\right], \quad r\ll 1,$$
$$\Delta h_p<0, \quad \Delta s_p<0, \quad T_c\ll T_p, \tag{88}$$

whereas the critical temperature $T_c$ depends on both $\epsilon_{\mathrm{FH}}$ and $r$,

$$T_c=2\epsilon_{\mathrm{FH}}\left\{1-\left(\frac{r}{2}\right)^{1/2}+\frac{3}{2}\left(\frac{r}{2}\right)+O\left[\left(\frac{r}{2}\right)^{3/2}\right]\right\}. \tag{89}$$

For small $r$, Eq. (89) simplifies to $T_c\simeq 2\epsilon_{\mathrm{FH}}(1-\phi_c)$, and this relation contrasts with Eq. (35) for the free association system where $T_c\simeq 2\epsilon_{\mathrm{FH}}$. The independence of $\phi_c$ on temperature and the emergence of a nonzero $\phi_c$, even at a very low $T$, accentuates another relevant difference between chemically initiated and free association polymerization processes. Equation (88) can be alternatively reexpressed in terms of the low temperature average chain length $L=2/r$, yielding

$$\phi_c=L^{-1/2}-L^{-1}+O(L^{-3/2}), \quad r\ll 1$$
$$\Delta h_p<0, \quad \Delta s_p<0, \quad T_c\ll T_p, \tag{90}$$

which is the (mean field) asymptotic result[27] for the critical composition of a high molecular weight polymer solution of polymerization index $L$.

The osmotic pressure is evaluated as

$$\frac{\Pi a^3}{k_BT}=-\ln(1-\phi_1^o-\phi_I)+\phi_1-\phi_1^o-(1/2)\phi_I$$
$$-\chi(\phi_1^o+\phi_I)^2, \tag{91}$$

which is equivalent to Eq. (6) of Paper III. The second virial coefficient $A_2$,

$$A_2=-\chi(1+r)^2+(1/2)(1+r)^2-(1/2)r(1-r)G, \tag{92}$$

is obtained by expanding the first two terms of Eq. (91) around $\phi_1^o\to 0$ and keeping $r=\phi_I/\phi_1^o$ constant. An alternative definition of $A_2$, that arises from expanding the terms of Eq. (91) around the $\phi\equiv\phi_1^o+\phi_I\to 0$ limit and keeping $\phi_I$ constant, is reported in Paper III. The third virial coefficient $A_3$, which is not considered in our previous paper,[3] is given by

$$A_3=(1/3)(1+r)^3-(1/2)r(1-r)[1-(3/2)r]G^2, \tag{93}$$

where $G$ is defined in Eq. (77).

## V. CRITICAL COMPARISON OF EQUILIBRIUM POLYMERIZATION MODELS

Although many characteristics of the equilibrium polymerization models described in the previous sections exhibit broad similarities, the presence of thermal activation or chemical initiation processes greatly affects the breadth of the polymerization transition, the rate $dL(T)/dT$ at which polymers grow as the temperature $T$ is varied, and the ultimate average length $L(T\ll T_p)$ of polymers far below the polymerization transition temperature $T_p$. In this section, we compare and contrast several basic thermodynamic properties to clarify the extent of their similarity. While the theory of Secs. II–IV applies for quite general cases of equilibrium polymerization, the present illustrative analysis is specialized to systems that polymerize upon cooling ($\Delta h_p<0, \Delta s_p<0$) and to stiff chains for comparison and consistency with the results summarized in Papers I–III. The more general treatment of systems containing semi-flexible polymer chains leads to much more complicated theoretical expressions, but to the same qualitative trends in thermodynamic behavior.

The free association, chemical initiation, and thermal activation models involve different numbers of essential parameters governing polymerization and phase separation. The simplest free association (F) model only requires specification of the enthalpy $\Delta h_p$ and entropy $\Delta s_p$ of polymerization. The initiation (I) model is described by an additional variable, the relative initiator concentration $r=\phi_I/\phi_1^o$, which is assumed to be constant and independent of the initial monomer concentration $\phi_1^o$. The thermal activation (A) model is determined by the specification of the enthalpy $\Delta h_a$ and entropy $\Delta s_a$ for the monomer activation process, in addition to the polymerization reaction parameters $\Delta h_p$ and $\Delta s_p$. Obviously, the specific thermodynamic properties predicted by each of these three models generally depend on $T$, the initial monomer concentation $\phi_1^o$, and the strength of the effective interaction $\epsilon_{\mathrm{FH}}$ (which within FH theory describes the variation of the effective monomer–solvent interaction parameter $\chi$ with temperature $T$).

Unless otherwise noted, the representative values $\Delta h_p=-35$ kJ/mol and $\Delta s_p=-105$ J/(mol K) are chosen for calculations illustrating and contrasting equilibrium polymerization in these three models. [These parameters are those determined from extensive experimental investigations of the poly($\alpha$-methylstyrene) living polymerization by Greer *et al.*[4,5]] To minimize the number of variables, the entropy of activation $\Delta s_a$ in the A model is taken as identical to the entropy of polymerization $\Delta s_p$ [$\Delta s_p=\Delta s_a=-105$ kJ/(mol K)] because these two quantities are anticipated to have comparable orders of magnitude in many systems. The initiator concentration $r$ for the I model is chosen as $r=0.0044$, which is the value utilized in former studies of poly($\alpha$-methylstyrene) solutions.[4,5] Finally, the enthalpy of activation $\Delta h_a$ is varied between the extreme limits of $\Delta h_a=0$ and $\Delta h_a=\Delta h_p$ corresponding to a relatively low and high equilibrium constant for activation, respectively. Consequently, the following text employs the notation of $\mathrm{A_{low}}\equiv\mathrm{A}(\Delta h_a=0)$ and $\mathrm{A_{high}}\equiv\mathrm{A}(\Delta h_a=\Delta h_p)$ to describe these relatively ''low activation'' and ''high activation'' limits. In the former $\mathrm{A_{low}}$ case, the majority of monomers remains as the nonactivated species $M_1$, and the polymer propagation reaction between the $M_1$ and $M_i$ ($i\geqslant 2$) species [see Eq. (38)] is favorable (for the above choices of $\Delta h_p$ and $\Delta s_p$), whereas in the latter $\mathrm{A_{high}}$ case, almost all monomers are converted into activated species $M_1^*$, which inhibits polymer growth because the propagation steps in Eqs. (37) and (38) involve unactivated monomers $M_1$. Note that this physical interpretation of the activated polymerization refers only to the polymerization reaction scheme defined by Eqs. (36)–

TABLE I. Values of parameters used in comparative analysis of equilibrium polymerization models.

| | Model | | | | |
|---|---|---|---|---|---|
| Parameter | F | $A_{low}$ | $A_{int}$ | $A_{high}$ | I |
| $\Delta h_p$ (kJ/mol) | −35 | −35 | −35 | −35 | −35 |
| $\Delta s_p$ [J/(mol K)] | −105 | −105 | −105 | −105 | −105 |
| $\Delta h_a$ (kJ/mol) | NA | 0 | −17.5 | −35 | NA |
| $\Delta s_a$ [J/(mol K)] | NA | −105 | −105 | −105 | NA |
| $r=\phi_I/\phi_1^o$ | NA | NA | NA | NA | 0.0044 |

(38), which is considered exclusively in our comparative analysis. [The alternative activated polymerization mechanism see Eqs. (39)–(41), which assumes the participation of activated monomers in the propagation steps, is mathematically isomorphic upon a redefinition of the free energy parameters.] In addition to the $A_{low}$ and $A_{high}$ models, an "intermediate activation model," $A_{int} \equiv A(\Delta h_a = \Delta h_p/2)$, is also included in some figures to illustrate how a moderate equilibrium constant for activation affects the polymerization process. Table I summarizes the parameters used in illustrative calculations for the basic models of equilibrium polymerization. The lattice coordination number is taken as $z=6$ (appropriate to a cubic lattice in three dimensions), and the effective interaction is $\epsilon_{FH}=302$ K, following the convention of Paper II.

### A. The average chain length *L* and extent of polymerization Φ

The average degree of polymerization $L$ of polymer chains is one of the most essential properties of equilibrium polymer solutions. Figures 1(a) and 1(b) display the variation of $L$ with $T$ (for a fixed $\phi_1^o$) and with $\phi_1^o$ (for a fixed $T$), respectively, for the $A_{low}$, $A_{int}$, $A_{high}$, F, and I models. Inspection of Figs. 1(a) and 1(b) reveals a substantial model dependence of $L$ for a given choice of the polymerization free energy parameters. The chain length $L$ diverges at low temperatures in the low activation model $A_{low}$, but saturates to a finite value $[L(T \ll T_p)=2/r]$ in the initiation model I for fixed nonzero $r$. ($L$ in the I model evidently diverges at low $T$ as $r \to 0^+$.) Neither a saturation effect ($L \to$ constant), nor a diverging behavior of $L$, occurs in the F, $A_{int}$, and $A_{high}$ models at low temperatures ($T \to 0^+$), however. For the $A_{high}$ model, chain growth at low $T$ is very limited, and we find $L(T \to 0^+)=1.2$, a magnitude that is indistinguishable from unity on the scale employed in Fig. 1(a). The high activation model $A_{high}$ resembles the initiation model I in the formal limit $r \to 1^+$ where $L(T \to 0^+)=2$. The free association model F, in which all particles *can* associate without restriction, corresponds approximately to the activation model with $\Delta h_a = \Delta s_a = 0$ (denoted as $A_o$), i.e., to a system with an equal probability for each monomer to be activated or unactivated. The $L(T)$ curves for the F and $A_o$ models are indistinguishable in Fig. 1(a), while other computed properties (e.g., the extent of polymerization) are close, but not identical. As discussed in Sec. II, $L$ diverges in the F model only as $T \to 0^+$, and the polymerization occurs

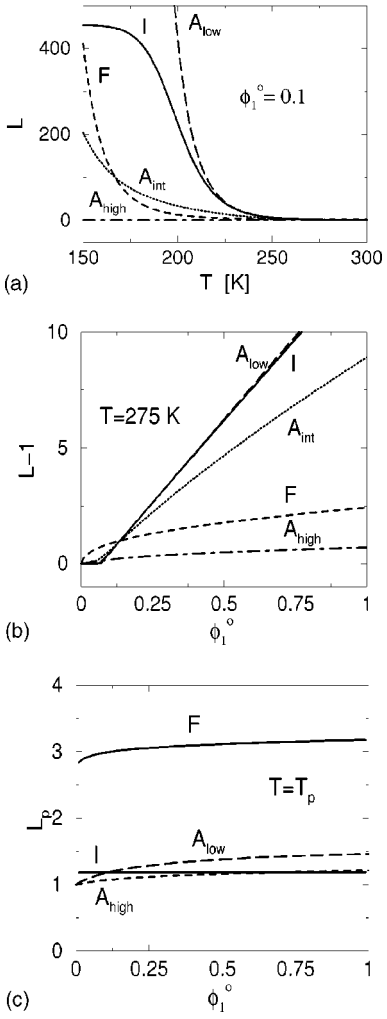


FIG. 1. (a) Average degree of polymerization $L$ as a function of temperature $T$ for the free association (F), thermal activation (A), and chemical initiation (I) models of equilibrium polymerization. The initial monomer concentration $\phi_1^o$ is fixed as 0.1. The three activation models $A_{low}$, $A_{high}$, and $A_{int}$ correspond to a low, high, and intermediate value of the equilibrium constant $K_a=\exp(-\Delta f_a/k_BT)$, respectively, where $\Delta f_a=\Delta h_a - T\Delta s_a$ is the free energy of activation. (Values of $\Delta h_a$ and $\Delta s_a$ for the three A models are given in Table I.) The same enthalpy $\Delta h_p=-35$ kJ/mol and entropy $\Delta s_p=-105$ J/(mol K) of polymerization are used for the F, I, and A models. The initiator concentration $r$ for the I model is chosen as $r=0.0044$. Unless otherwise noted, the same parameters ($\Delta h_p$, $\Delta s_p$, $\Delta h_a$, $\Delta s_a$, and $r$) are employed in all subsequent figures, and all figures refer to polymerization upon cooling. (b) Average degree of polymerization $L-1$ at $T=275$ K as a function of initial monomer concentration $\phi_1^o$ for the F, I, $A_{low}$, $A_{high}$, and $A_{int}$ models. (c) The averaged degree of polymerization $L_p$ at the polymerization temperature $T_p$ as a function of $\phi_1^o$ for the same models as in Figs. 1(a) and 1(b).

gradually over a very wide range of $T$, as found in the A model with a rather high equlibrium constant $K_a = \exp(-\Delta f_a/k_BT)$.

The concentration dependence of $L$ at a fixed $T$ [see Fig. 1(b)] is likewise sensitive to the mode of association. The commonly noted[23–25] $(\phi_1^o)^{1/2}$ scaling of $L$ emerges from Fig. 1(b) as a representative feature of the F, $A_{int}$, and $A_{high}$ models. On the other hand, $L$ is nearly *linear* in $\phi_1^o$ (over an appreciable range of $\phi_1^o$) for both the I and $A_{low}$ models.[41] The "critical polymerization concentration" (cpc) $(\phi_1^o)^*$, defined as the value of $\phi_1^o$ at which $L-1$ extrapolates to zero,[1] does not appear at any finite $T$ for either the F and $A_{high}$ models. In contrast, this critical concentration exists for both the I and $A_{low}$ models, where we find $(\phi_1^o)^* \simeq 0.06$ at $T=275$ K. The absence of a well-defined cpc in the F and $A_{high}$ models arises from the extremely broad nature of the polymerization transition in these two models. Figures 1(a) and 1(b) clearly indicate that the presence of activation and initiation processes can dramatically influence not only the rate $dL(T)/dT$ at which chains grow with $T$, but also the magnitude of the variation of $L$ with $\phi_1^o$ (see also Paper I) and the sharpness of the polymerization transition.

The average chain length $L$ is not large at the polymerization transition temperature $T_p$ (defined by the maximum in the specific heat $C_V$ as a function of $T$) and is sensitive to the details of the equilibrium polymerization model. Figure 1(c) displays $L$ at $T_p$ $[L_p \equiv L(T_p)]$ as a function of the initial monomer concentration $\phi_1^o$ for the models compared in Figs. 1(a) and 1(b). $L_p$ is remarkably insensitive to $\phi_1^o$ and remains close to unity in all the models considered, except for the F model where $L_p \simeq 3$. We expect this near constancy of $L$ at $T_p$ to be a general feature of systems undergoing equilibrium polymerization. Thus, it should be possible to locate the transition by comparing $L$ to these characteristic $L_p$ values. The use of this procedure requires knowledge of which polymerization model applies to a given physical system, but it is sometimes unclear whether or not activation processes are involved.

The extent of polymerization $\Phi$ plays the role of an "order parameter" describing the degree to which the polymerization transition is completed (in general, these transitions are "rounded transitions" as described in Paper III). Figure 2(a) presents $\Phi$ for fixed $\phi_1^o = 0.1$, showing that $\Phi$ changes sharply with $T$ for the I, $A_{low}$, and $A_{int}$ models, but varies in a more gradual manner for the F and $A_{high}$ models. Interestingly, $\Phi$ in the $A_{high}$ model does not approach unity at low $T$ because of the presence of a large concentration of activated monomers $M_1^*$. For low $T$, the large negative value of $\Delta f_a = \Delta h_a - T\Delta s_a$ in the $A_{high}$ model implies that the activation reaction in Eq. (36) proceeds almost to completion, leaving only a very small concentration of nonactivated species $M_1$. Consequently, this large concentration of activated monomers cannot be significantly diminished through the dimerization and polymer propagation processes, despite a favorable free energy of polymerization $\Delta f_p$ $(\Delta f_p = \Delta h_p - T\Delta s_p \ll 0)$ since the unactivated monomers $M_1$ are reactants in both these processes [see Eqs. (37) and (38)]. The small $\Phi(T \ll T_p) \simeq 0.3$ for the $A_{high}$ model is consistent with the minimal degree of polymerization $L$ occurring at low $T$ in this model, $L(T \ll T_p) \simeq 1.2$ [see Fig. 1(a)]. The $\Phi(T)$ curves in Fig. 2(a) exhibit inflection points $(\partial^2\Phi/\partial T^2)|_{\phi_1^o} = 0$ at nearly the same $T$ for the I and $A_{low}$ models, and the inflection points shift gradually to higher temperatures for the $A_{int}$, F, and $A_{high}$ models (in this sequence). The shift does not scale uniformly with the magnitude of $\Delta h_a$, however. The free association model yields a very broad polymerization transition in which polymerization occurs even at $T \gg T_p$, and, hence, $\Phi$ for the F model exceeds $\Phi$ in the I and $A_{low}$ models over a wide range of $T$ and $\phi_1^o$ [see Fig. 2(a)].

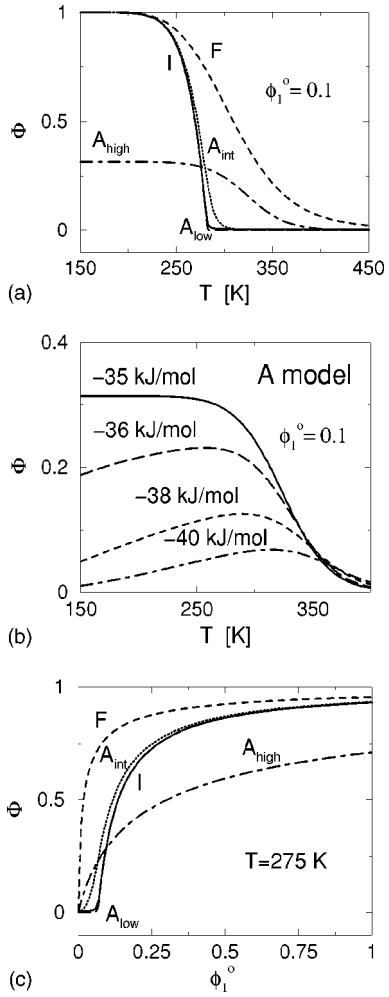


FIG. 2. (a) Extent of polymerization $\Phi$ as a function of temperature $T$ for the F, I, $A_{low}$, $A_{high}$, and $A_{int}$ models. The initial monomer monomer concentration $\phi_1^o$ is fixed at 0.1. (b) Extent of polymerization $\Phi$ as a function of temperature $T$ for the activated association model A. Different curves correspond to different values of the enthalpy $\Delta h_a$ of monomer activation. The initial monomer concentration $\phi_1^o$ is fixed as 0.1. $\Phi(T)$ exhibits a maximum when $|\Delta h_a| > |\Delta h_p|$. (c) Extent of polymerization $\Phi$ at a fixed temperature $T=275$ K as a function of initial monomer concentration $\phi_1^o = 0.1$ for the F, I, $A_{low}$, $A_{high}$, and $A_{int}$ models of equilibrium polymerization.

Decreasing the magnitude of $\Delta h_a$ introduces a nontrivial *competition* between the polymerization and activation processes that may lead to unique behaviors. Figure 2(b) shows that this competition produces a maximum in $\Phi(T)$ for fixed $\phi_1^o$ as a function of $T$ that is more pronounced as the magnitude of $(\Delta h_a - \Delta h_p)$ becomes more negative. Additional calculations indicate that the height of a maximum in $\Phi(T)$ also grows when $|\Delta s_a|$ exceeds $|\Delta s_p|$. Equation (59) pro-

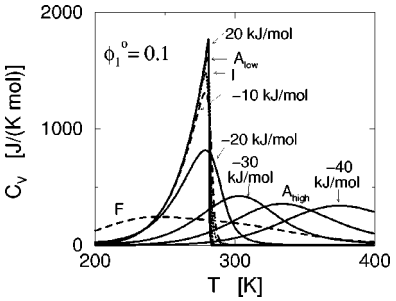


FIG. 3. Temperature dependence of the specific heat $C_V$ in various models of equilibrium polymerization for the fixed initial monomer concentration $\phi_1^o = 0.1$. The curves for $C_V(T)$ corresponding to activation models other than $A_{low}$ and $A_{high}$ are labeled by the enthalpy of activation $\Delta h_a$.

vides general conditions for the vanishing of the temperature derivative of $\Phi$, i.e., for the maximum in $\Phi(T)$. A maximum for $\Phi(T)$ has been observed recently for the polymerization of G-actin.[42] A nonmonotonic variation of $\Phi$ with $T$ is a good indicator of the presence of activation processes in the polymerization.

Figure 2(c) depicts $\Phi(T = 275\ \mathrm{K})$ as a function of the initial monomer concentration $\phi_1^o$, exhibiting $\Phi$ from a different perspective than in Fig. 2(a). The same $T$ is chosen in Figs. 1(b) and 2(c) for consistency. The extent of polymerization $\Phi(T = 275\ \mathrm{K})$ increases sharply with $\phi_1^o$ when $\phi_1^o$ exceeds $(\phi_1^o)^*$ in the I and $A_{low}$ models, but grows from a vanishing concentration $(\phi_1^o = 0)$ for the F, $A_{int}$, and $A_{high}$ models. The changes of $\Phi(\phi_1^o)$ are more gradual in the high activation $A_{high}$ model, while the rise of $\Phi$ is sharp for the F model. As discussed earlier,[3] transition rounding is responsible for the absence of a cpc in the F, $A_{int}$, and $A_{high}$ models.

### B. Specific heat $C_V$ and polymerization temperature $T_p$

The specific heat $C_V$ provides another characteristic signature of the polymerization transition. The polymerization transition in the I and A models, respectively, is known to reduce to a second-order phase transition as $r \to 0^+$ or as the activation equilibrium constant approaches zero.[17–19] Figure 3 depicts the specific heat $C_V$ at a fixed initial monomer concentration $\phi_1^o = 0.1$ as a function of $T$ for the I, F, and for several A models (specified by values of $\Delta h_a$), including those defined previously as $A_{low}$ and $A_{high}$. All the other free energy parameters are the same as in Figs. 1 and 2. The sharp polymerization transition for the $A_{low}$ and I model in Fig. 3 contrasts with a very broad maximum in $C_V$ for the $A_{high}$ and F model. When $\Delta h_a$ is less than $-20$ kJ/mol, a significant broadening of the transition appears (and increases with a more negative $\Delta h_a$). Moreover, the polymerization temperature $T_p$ [corresponding to the maximum of $C_V(T)$] increases substantially as $\Delta h_a$ becomes more negative [see also Fig. 4(a)]. For instance, a change in $\Delta h_a$ from $-20$ to $-40$ kJ/mol produces an increase of $T_p$ by almost 100 K. On the other hand, $T_p$ changes slightly when $\Delta h_a$ becomes less negative than $-20$ kJ/mol, but these slight shifts in $T_p$ with an increase in $\Delta h_a$ beyond $-20$ kJ/mol are accompanied by significant sharpening of the transition and the $C_V$ maximum.

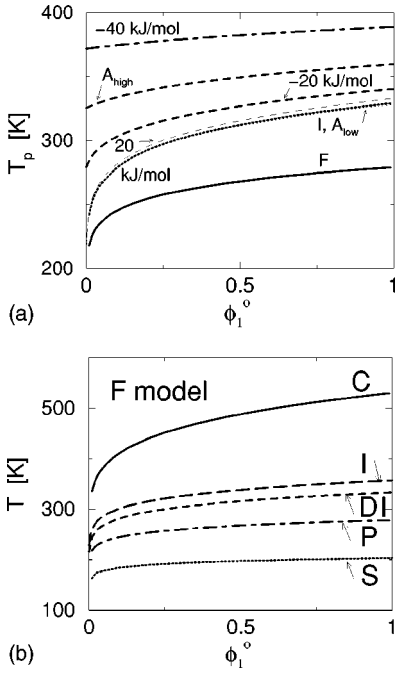


FIG. 4. (a) Concentration dependence of the polymerization temperature $T_p$. Models are the same as in Fig. 3. (b) The saturation (S), polymerization (P), Dainton–Ivin equation (DI), inflection point $(\partial^2\Phi/\partial T^2)|_{\phi_1^o} = 0$ (I), and crossover (C) lines for the free association F model.

In summary, Fig. 3 demonstrates that both the activation and initiation processes can also substantially influence the breadth of the polymerization transition and its location.

The sensitivity of $T_p$ to the mode of equilibrium polymerization has important ramifications on methods for determining the free energy parameters from the experimental dependence of $T_p$ on the initial monomer concentration $\phi_1^o$. Figure 4(a) displays the polymerization transition lines $T_p(\phi_1^o)$ for the F and I models and for a few activation models, including those designated as $A_{low}$ and $A_{high}$. The same $\Delta h_a$ values are used in Figs. 3 and 4(a), while all the other energy parameters are fixed as in Figs. 1 and 2. The I and $A_{low}$ model polymerization lines are almost indistinguishable on the scale of Fig. 4(a), lying close to the well-known Dainton–Ivin (DI) equation line. On the other hand, the F model transition curve is located, on average, at least 50 K *below* this "classical" estimate of $T_p$. Decreasing $\Delta h_a$ from $\Delta h_a = 0$ strongly shifts the transition curve to higher temperatures over the whole range of $\phi_1^o$, and the $\phi_1^o$ dependence of $T_p$ becomes weaker for more negative $\Delta h_a$.

There is a common view that the DI equation provides a good estimate of $T_p$ for equlibrium polymerization systems (subject to the assumption of ideal solution conditions),[33,43] and indeed this classic estimate to $T_p$ proves to be accurate for the I and $A_{low}$ models. For example, Paper I demonstrates that the DI estimate of $T_p$ differs by only 10–15 K from the actual $T_p$ for the I model systems with $r$ as large as $r = 0.1$. On the other hand, Eq. (24) can be grossly in error for other equilibrium polymerization models. Figure 4(b) delineates this failure for the F model by displaying the polymerization line, the inflection point $(\partial^2\Phi/\partial T^2)|_{\phi_1^o} = 0$ line, and the DI equation line for this model. As mentioned before, the

first two curves become identical for both the $A_{low}$ and I models [see also Eq. (84)] and coincide with the third curve provided that $r \ll 1$, while this correspondence is absent for the F model or the activation model with a rather high activation equilibrium constant $K_a$. As shown in Fig. 4(b), large differences (on the order of 60–80 K over almost the full range of $\phi_1^o$) emerge in the F model between the polymerization temperature (corresponding to the maximum of $C_V$) and the temperature at which the derivative $(\partial^2\Phi/\partial T^2)|_{\phi_1^o}$ vanishes. The inflection point line, which is sometimes used to estimate[38] $T_p$, lies relatively close to the DI curve for the F model [see Fig. 4(b)]. For completeness, Fig. 4(b) depicts two additional characteristic curves. The lower (''saturation line'') corresponds to the loci of temperatures where the configuration entropy $S(T)$ (fluid entropy apart from the vibrational contribution) of the free association system approaches within 5% its low temperature limiting value, and the upper (''crossover line'') denotes the loci where the extent of polymerization is 5% greater than its high $T$ limiting value $\Phi(T \to \infty)$.[1] For systems that polymerize upon cooling, these transition lines roughly delineate where the polymerization transition region effectively ends and begins, respectively. A large difference between the crossover and saturation temperatures reflects the broadness of the polymerization transition for the F model. The elevated crossover temperatures for the F model are consistent with a long high $T$ tail for the extent of polymerization $\Phi(T)$ in Fig. 2(a).

The difficulties in determining the true free energy parameters governing the polymerization process from experimental data for $T_p$ are mitagated by our finding that the DI equation often can be forced to ''fit'' polymerization lines as in Fig. 4(b), provided that the free energy parameters are ''rescaled'' from their true values. This ''renormalization'' of parameters seems to exhibit regularities that we are currently studying and that should allow a *correct estimation* of $\Delta h_p$ and $\Delta s_p$ from data for $T_p$. Our findings also explain the apparent phenomenological ''success'' of the DI equation in situations where it actually fails to apply. Since the behavior of these ''shifts'' in the polymerization model parameters (between those representing the actual systems and those inferred by application of the DI equation to data for $T_p$) are rather involved, we defer discussion of this important problem to a separate paper.

### C. Competition between polymerization and phase separation

Papers II and III indicate the existence of a strong coupling between equilibrium polymerization and phase separation for ''living polymerization'' systems (I model). These papers demonstrate that a decrease in the enthalpy of polymerization $\Delta h_p$ generally leads to an increased critical temperature $T_c$, a more asymmetric phase diagram, and a decreasing critical composition $\phi_c$. These general trends are obtained for a *fixed* strength $\epsilon_{FH}$ of the effective van der Waals interaction $\chi$ and for a fixed entropy of polymerization $\Delta s_p$, and are illustrated in Fig. 1 of Paper II. A different behavior for $T_c$ and $\phi_c$ emerges for the I model, however, when the enthalpy $\Delta h_p$ and entropy of polymerization $\Delta s_p$ are fixed, but $\epsilon_{FH}$ is instead varied. [See Fig. 5(a), which extends the studies from Paper II]. The critical temperature $T_c$ grows monotonically with $\epsilon_{FH}$ in a nontrivial fashion. In the low $\epsilon_{FH}$ regime $[0 < \epsilon_{FH} < \epsilon_{FH}^{(1)} = (1/2)\Delta h_p/\Delta s_p]$, $T_c$ lies below $T_p$ and nearly coincides with the $T_c$ for high molecular weight polymer solutions, i.e., $T_c = 2\epsilon_{FH}$. For intermediate $\epsilon_{FH}$ $[(1/2)\Delta h_p/\Delta s_p < \epsilon_{FH} < 2\Delta h_p/\Delta s_p]$, $T_c$ approaches the DI estimate of the polymerization temperature $T_p^{(o)}$. When $\epsilon_{FH}$ exceeds another ''critical'' value $\epsilon_{FH}^{(2)} = 2\Delta h_p/\Delta s_p$, the critical temperature $T_c$ surpasses $T_p$ and becomes linear in $\epsilon_{FH}$ with a proportionality coefficient of 1/2, thus following the critical temperature $T_c$ for a monomer–solvent system in which no polymerization is present, i.e., $T_c = (1/2)\epsilon_{FH}$. These two critical values of $\epsilon_{FH}$, $\epsilon_{FH}^{(1)} = (1/2)\Delta h_p/\Delta s_p$ and $\epsilon_{FH}^{(2)} = 2\Delta h_p/\Delta s_p$, correspond to the intersections of the absolute polymerization transition temperature [i.e., $T_p(\phi_1^{(o)} = 1)$] with $T_c$ and with the theta temperature $T_\theta$, respectively, as described in Papers II and III and in the following. The variation of $\phi_c$ (for constant $\Delta h_p$ and $\Delta s_p$) with $\epsilon_{FH}$ is also instructive [see Fig. 5(b)]. The critical composition is independent of $\epsilon_{FH}$ when $\epsilon_{FH} < (1/2)\Delta h_p/\Delta s_p$ (and depends only on $r$), but then $\phi_c$ grows with $\epsilon_{FH}$ and finally exceeds the monomer solution value of 1/2. After achieving a maximum ($\simeq 0.7$ for $r = 0.0044$), $\phi_c$ drops sharply to a limiting value departing slightly from 1/2 (due to a nonzero $r$) when $\epsilon_{FH} > 2\Delta h_p/\Delta s_p$. Moreover, a more careful examination of Fig.

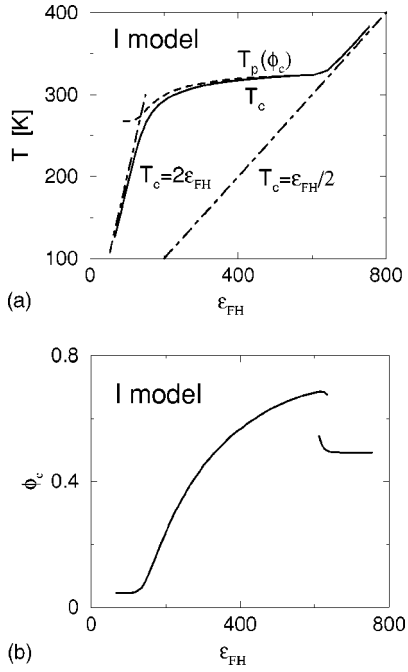


FIG. 5. (a) The critical temperature $T_c$ (solid line) as a function of the strength of effective monomer–solvent interaction $\epsilon_{FH}$ $(\chi = \epsilon_{FH}/T)$ for the I model. The dashed line denotes the ideal Dainton–Ivin polymerization temperature calculated at the critical composition $(\phi_1^o)^{(c)} \equiv \phi_c$. The dot-dashed lines indicate the asymptopic behavior of $T_c$ for infinite molecular mass polymer solutions $(T_c = 2\epsilon_{FH})$ and for monomer–solvent systems $(T_c = \epsilon_{FH}/2)$. (b) The critical temperature $\phi_c$ as a function of the strength of effective monomer–solvent interaction $\epsilon_{FH}$ $(\chi = \epsilon_{FH}/T)$ for the I model. Two critical points are present over the narrow range 611 K$< \epsilon_{FH} <$634 K.

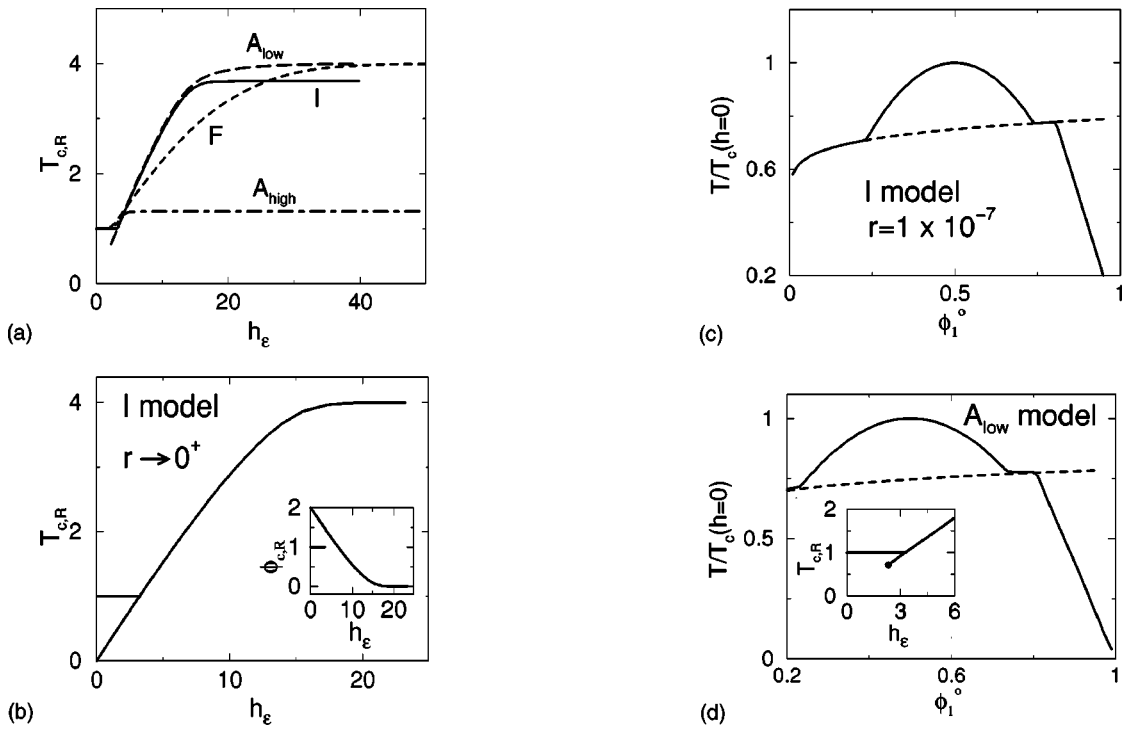


FIG. 6. (a) The reduced critical temperature $T_{c,R}\equiv T_c/T_c(\Delta h_p=0)$ as a function of the dimensionless interaction $h_\epsilon\equiv(|\Delta h_p|/R)/(2\epsilon_{\mathrm{FH}})$ for the F, I, $A_{\mathrm{low}}$, and $A_{\mathrm{high}}$ models. (b) The reduced critical temperature $T_{c,R}\equiv T_c/T_c(\Delta h_p=0)$ as a function of the dimensionless interaction $h_\epsilon\equiv(|\Delta h_p|/R)/(2\epsilon_{\mathrm{FH}})$ for the I model in the $r\to 0^+$ limit. The inset illustrates the variation of the reduced critical composition $\phi_{c,R}\equiv\phi_c/\phi_c(\Delta h_p=0)$ with $h_\epsilon$. (c) Illustrative example of a phase diagram (spinodal curve) with two critical points for the I model in the $r\to 0^+$ limit for a fixed dimensionless interaction $h_\epsilon\equiv(|\Delta h_p|/R)/(2\epsilon_{\mathrm{FH}})=2.5$. The dashed curve indicates the polymerization line which coincides with the spinodal over certain ranges of $\phi_1^o$ and passes through a second critical point. (d) A representative spinodal (solid curve) with two critical points in the $A_{\mathrm{low}}$ model ($K_a=3.28\times 10^{-6}$) for the dimensionless interaction $h_\epsilon\equiv(|\Delta h_p|/R)/(2\epsilon_{\mathrm{FH}})=2.5$. The dashed curve represents the polymerization line which intersects the spinodal at the second critical point occurring at $\phi_1^o>1/2$. The inset shows the reduced critical temperature $T_{c,R}\equiv T_c/T_c(\Delta h_p=0)$ as a function of $h_\epsilon$ for the same model. The black dot is placed at the termination of the second critical point.

5(b) reveals that there are *two* critical points over the narrow range 611 K$<\epsilon_{\mathrm{FH}}<$634 K for $r=0.0044$. The two critical points have similar values of $T_c$, but quite different $\phi_c$. The occurrence of the *second* critical point is just apparent in Fig. 5(b), but in other instances (see the following), the bifurcation into two distinct critical points is quite evident.

While Fig. 1 of Paper II and Figs. 5(a) and 5(b) of the present paper illustrate the coupling between polymerization and phase separation from two different perspectives (i.e., for fixed $\epsilon_{\mathrm{FH}}$ and for fixed $\Delta h_p$, respectively), our more recent analysis indicates that these two perspectives can be combined by considering the reduced critical parameters $T_{c,R}\equiv T_c/T_c(\Delta h_p=0)$ and $\phi_{c,R}\equiv\phi_c/\phi_c(\Delta h_p=0)$ which do not depend separately on $\Delta h_p$ and $\epsilon_{\mathrm{FH}}$, but only on their combination $(\Delta h_p/R)/\epsilon_{\mathrm{FH}}$ (where $R$ is the gas constant). This finding is valid for *all* the models investigated in the present paper. The normalization of $\phi_c$ by the corresponding value in the absence of polymerization is, however, redundant since $\phi_c$ is itself (in contrast to $T_c$) a function of $\Delta h_p/\epsilon_{\mathrm{FH}}$ (and $\Delta s_p$), but a reduced $\phi_c$ is introduced for consistency with the normalization of $T_c$. Figures 6(a)–8 compare the critical properties between the different models described in Secs. II–IV as functions of this dimensionless "sticking energy" $h_\epsilon\equiv(|\Delta h_p|/R)/(2\epsilon_{\mathrm{FH}})$. All other adjustable parameters (i.e., $\Delta s_p$, $\Delta h_a$, $\Delta s_a$, and $r$) are fixed as in former figures, and $\Delta h_p<0$ is chosen since we constrain the discussion to polymerization upon cooling.

Figure 6(a) presents the relative critical temperature $T_{c,R}$ as a function of $h_\epsilon$ for the I, $A_{\mathrm{low}}$, $A_{\mathrm{high}}$, and F models. All the curves for $T_{c,R}(h_\epsilon)$ in Fig. 6(a) exhibit two plateau regions in which $T_{c,R}(h_\epsilon)$ is independent of $h_\epsilon$. While these plateaus represent a characteristic feature of equilibrium polymerization, their magnitudes vary between the different models. The critical temperature $T_c(h_\epsilon)$ increases substantially from its "bare" value $T_c(\Delta h_p=0)$, or, in other words, $T_{c,R}$ departs from unity when $h_\epsilon$ exceeds a critical value $h_{\epsilon,1}$ that depends rather weakly on the model. As $h_\epsilon$ surpasses another "critical" value $h_{\epsilon,2}$, the critical temperature $T_c$ is found to saturate. Apparently, $T_c$ cannot exceed the theta temperature $T_\theta^{(0)}\equiv T_\theta(\Delta h_p=0)$ in the absence of polymerization (the $T$ at which $A_2$ vanishes). Moreover, the second "critical" reduced "sticking energy" $h_{\epsilon,2}$ is strongly model dependent. While $T_{c,R}$ approaches the relative theta temperature $T_{\theta,R}^{(0)}\equiv T_\theta(\Delta h_p=0)/T_c(\Delta h_p=0)=4$ for the $A_{\mathrm{low}}$ and F models (albeit in a much slower fashion in the latter case), the limiting value of $T_{c,R}$ differs from 4 by less than 10% for the I model (due to nozero $r$), but it is significantly lower ($T_{c,R}\simeq 1.35$) for the $A_{\mathrm{high}}$ model. This different behavior for the $A_{\mathrm{high}}$ model accords with the small average degree of

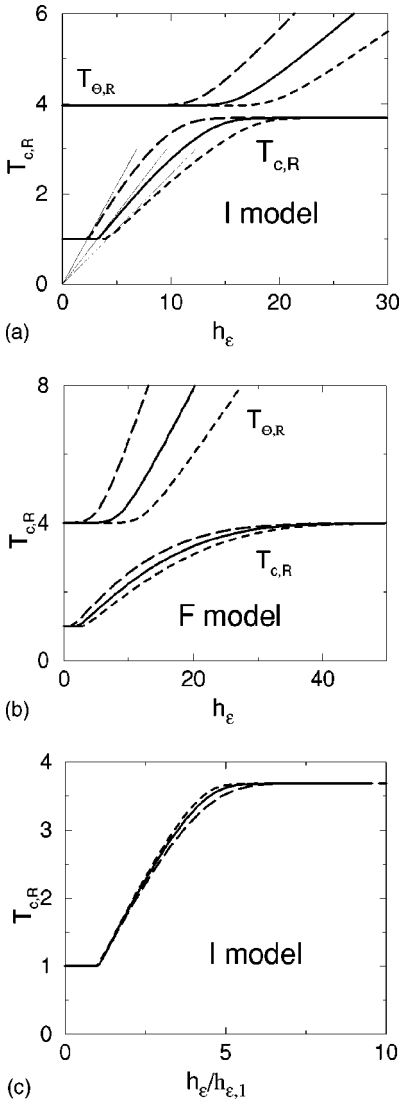


FIG. 7. (a) The reduced critical temperature $T_{c,R}\equiv T_c/T_c(\Delta h_p=0)$ as a function of the dimensionless interaction $h_\epsilon\equiv(|\Delta h_p|/R)/(2\epsilon_{\mathrm{FH}})$ for the I model with a nonvanishing $r=0.0044$. Different curves correspond to different values of the polymerization entropy $\Delta s_p$. [The long-dashed, solid, and short-dashed curves refer to $\Delta s_p=-75$, $-105$, and $-135$ J/(mol K), respectively.] Also displayed is the reduced theta temperature $T_{\theta,R}\equiv T_\theta/T_c(\Delta h_p=0)$ to emphasize that $T_c$ never exceeds $T_\theta$. The thin solid lines represent the absolute polymerization temperatures $T_p^*$ divided by $T_c(\Delta h_p=0)$ for consistency with the other curves. (b) The reduced critical temperature $T_{c,R}\equiv T_c/T_c(\Delta h_p=0)$ as a function of the dimensionless interaction $h_\epsilon\equiv(|\Delta h_p|/R)/(2\epsilon_{\mathrm{FH}})$ for the F model. Different curves correspond to different values of the polymerization entropy $\Delta s_p$. [The long-dashed, solid, and short-dashed curves refer to $\Delta s_p=-75$, $-105$, and $-135$ J/(mol K), respectively.] Also displayed is the reduced theta temperature $T_{\theta,R}\equiv T_\theta/T_c(\Delta h_p=0)$ for the same values of $\Delta s_p$. (c) The reduced critical temperature $T_{c,R}\equiv T_c/T_c(\Delta h_p=0)$ as a function of $h_\epsilon/h_{\epsilon,1}$ where $h_{\epsilon,1}=(1/4)(|\Delta s_p|/R)$. The long-dashed, solid, and short-dashed curves refer to $\Delta s_p=-75$, $-105$, and $-135$ J/(mol K), respectively. The sensitivity of $T_{c,R}$ to $\Delta s_p$ diminshes significantly when $T_{c,R}$ is plotted vs $h_\epsilon/h_{\epsilon,1}$.

polymerization $L$ at $T_c$ [see Fig. 1(a)], precluding $T_{c,R}$ from being close to $T_{\theta,R}^{(0)}$ for large $h_\epsilon$. (These trends are comparable with FH theory predictions for polymer solutions where $T_{\theta,R}$ ranges monotonically from 4 in the unpolymerized monomer–solvent system to unity for an infinite molecular weight polymer solution.) Figure 6(a) also shows that

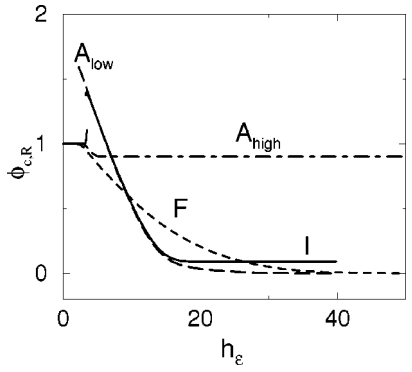


FIG. 8. The reduced critical composition $\phi_{c,R}\equiv\phi_c/\phi_c(\Delta h_p=0)$ as a function of the dimensionless "sticking energy" $h_\epsilon\equiv(|\Delta h_p|/R)/(2\epsilon_{\mathrm{FH}})$ for the F, I, $A_{\mathrm{low}}$, and $A_{\mathrm{high}}$ models.

two critical points coexist for the low activation model over a small range of $h_\epsilon$ ($2.31\leqslant h_\epsilon\leqslant 3.29$). As mentioned earlier, two critical points also appear for the I model ($r=0.0044$), but the range of $h_\epsilon$ is small ($3.32\leqslant h_\epsilon\leqslant 3.44$), so that the presence of both critical temperatures is almost indistinguishable on the scale of Fig. 6(a). Indeed, we did not even notice these multiple critical points in our previous Papers II and III.[44]

This fascinating multiple critical point phenomenon becomes pronounced in the limit of a very low activation equilibrium constant or of a low concentration of chemical initiators, where the polymerization transition approaches a second-order phase transition.[17] Figure 6(b) displays $T_{c,R}$ and $\phi_{c,R}$ as a function of $h_\epsilon$ for the I model in the $r\to 0^+$ limit. Both $T_{c,R}(h_\epsilon)$ and $\phi_{c,R}(h_\epsilon)$ are double-valued for $h_\epsilon<h_\epsilon^*$, and these critical parameters become unique above the bifurcation point. This behavior can be understood by analyzing the coupling between polymerization and phase separation in the "weak sticking energy" regime ($h_\epsilon<h_\epsilon^*\simeq 3.3195$).[45]

Figure 6(c) presents a representative spinodal curve for $h_\epsilon=2.5$ and $r=1\times 10^{-7}$ (solid curve) and the corresponding polymerization transition line $T_{p,R}$ (dashed line). The $T_{p,R}$ curve is a line of second-order phase transitions in the $r\to 0^+$ limit.[17] The critical point above the polymerization line ($T_{c,R}=1$) has its origin in the monomer–solvent phase separation in the absence of polymerization. The polymerization transition that occurs at $T_p<T_c(\Delta h_p=0)$ apparently distorts the phase boundary and leads to the appearance of the second critical point in the high concentration regime. More specifically, the polymerization line intersects the rightmost branch of the spinodal at a critical point.[19–21,46] The intersection of the polymerization line with the rightmost branch of the spinodal curve occurs at a temperature lower that the critical temperature $T_c(\Delta h_p=0)$ for the monomer–solvent mixture and at a composition larger than the critical composition $\phi_c=1/2$ of this reference system, explaining the trends in the variation of $\phi_c$ and $T_c$ with $h_\epsilon$. At the critical sticking energy $h_\epsilon^*$, the second critical point finally "absorbs" the remnants of the monomer–solvent critical point and shifts to temperatures higher than $T_c(\Delta h_p=0)$ and to compositions smaller that 1/2, as would be expected for a polymer solution of increasing molecular weight

[see Fig. 6(b)]. Essentially, the same trends are found for the A model in the limit of a vanishing activation equilibrium constant, where the polymerization line is also a line of second-order phase transitions.[17–19] Figure 6(d) provides an illustrative spinodal curve in the $A_{low}$ model ($K_a=3.28\times10^{-6}$) for the same value of $h_\epsilon=2.5$ as in Fig. 6(c), while the inset depicts $T_{c,R}$ as a function of $h_\epsilon$ for this model. Increasing $r$ (or $K_a$) leads to the ''rounding'' and finally to the disappearance of the second critical point. This second critical point *ceases to exist* below a critical value of $h_\epsilon$ (dependent on $r$ or $K_a$), where the polymerization transition becomes too ''weak'' to perturb the monomer–solvent phase separation [see inset to Fig. 6(d)].

The entropy of polymerization $\Delta s_p$ has been treated so far as a *fixed* parameter. This quantity, however, exerts a large influence on the critical behavior of associating fluids, and we now briefly discuss some essential aspects of this dependence. The entropy $\Delta s_p$ significantly affects the rate at which $T_{c,R}(h_\epsilon)$ varies between the two plateaus at large and small $h_\epsilon\equiv(|\Delta h_p|/R)/(2\epsilon_{FH})$. This phenomenon is illustrated in Figs. 7(a) and 7(b) for the I and F models, respectively, where $T_{c,R}$ and $T_{\theta,R}\equiv T_\theta/T_c(\Delta h_p=0)$ are presented for three different values of $\Delta s_p$ ranging from $-75$ J/(mol K) to $-135$ J/(mol K). A smaller (i.e., more negative) $\Delta s_p$ in Figs. 7(a) and 7(b) produces a weaker dependence of both $T_c(h_\epsilon)$ and $T_\theta(h_\epsilon)$ on $h_\epsilon$, and this apparently general trend extends to all the models considered. Figure 7(a) also includes the *absolute polymerization temperature* $T_p^*$ [reduced by $T_c(\Delta h_p=0)$ for consistency with the other transition curves] as the thin solid lines in Fig. 7(a). The importance of this reference polymerization temperature can be realized by noticing that the intersection of the $T_{p,R}^*(h_\epsilon)\equiv T_p^*/T_c(\Delta h_p=0)$ line with the $T_{c,R}(h_\epsilon)$ curve coincides with the first ''critical'' interaction $h_{\epsilon,1}$. This intersection point also corresponds to the end of the first plateau in Fig. 7(a). Recall that the DI equation becomes exact in the $r\to0^+$ limit and remains a good approximation even for $r=0.0044$ in the I model, so that $T_p^*\simeq\Delta h_p/\Delta s_p$ [see Eq. (24)]. Thus, $h_{\epsilon,1}$ is determined exclusively by the polymerization entropy $\Delta s_p$ and equals $h_{\epsilon,1}=(1/4)(|\Delta s_p|/R)$ for the I model in the limit of small initiator concentration ($r\to0^+$). More generally, this estimate of $h_{\epsilon,1}$ provides a rough approximation for the other equilibrium polymerization models [see Fig. 6(a)]. Figure 7(c) demonstrates that rescaling $h_\epsilon$ by $h_{\epsilon,1}$ reduces the $T_{c,R}(h_\epsilon)$ data of Fig. 7(a) to nearly a ''universal'' curve $T_{c,R}(h_\epsilon/h_{\epsilon,1})$ that is even relatively insensitive to $\Delta s_p$. An accurate extension of the same type of analysis to estimate $h_{\epsilon,1}$ for the F and A models requires a tedious calculation of $T_p$ to determine an appropriate expression to replace the DI equation.[47]

Differences in the variation of $T_c(h_\epsilon)$ between diferent equilibrium polymerization models in Figs. 6 and 7 are supplemented with a description of the corresponding changes in $\phi_c$ to fully elucidate the physics of the competition between polymerization and phase separation. Figure 8 depicts the variation of the reduced critical composition $\phi_{c,R}\equiv\phi_c/\phi_c(h_\epsilon=0)$ with the dimensionless interaction $h_\epsilon$ for the F, I, $A_{low}$, and $A_{high}$ models. The variable $\phi_{c,R}$ does not depart appreciably from unity for all the models when $h_\epsilon$ is small. In the F model, $\phi_{c,R}$ slowly and monotonically aproaches zero as $h_\epsilon$ increases, but it drops rapidly to a constant $\simeq0.92$ in the $A_{high}$ model. As already noted, the limited polymerization in the $A_{high}$ model is responsible for the saturation of the reduced critical temperature $T_{c,R}$ to a value of 1.35. The same feature leads to a minimal decrease of $\phi_c$ from its symmetric mixture value of 1/2 in the absence of polymerization. A much more complicated dependence of $\phi_{c,R}$ on $h_\epsilon$ emerges, however, from Fig. 8 for the I and $A_{low}$ models. As discussed earlier and indicated in Figs. 6(b)–6(d), these two models exhibit two critical points over a restricted range of $h_\epsilon$, which effectively results for a nonvanishing $r$ (or for a small activation equilibrium constant) in the apparent ''jump'' of $\phi_{c,R}$ in Fig. 8. The main difference between the I and $A_{low}$ models lies, however, in the behavior of $\phi_{c,R}$ in the range of large $h_\epsilon$, where $\phi_{c,R}$ of the $A_{low}$ model approaches zero, whereas $\phi_{c,R}$ for the I model saturates to a constant $\simeq0.09$, according well with the estimation of $\phi_c$ based on our asymptotic analysis for $r\ll1$. [Equation (88) for $r=0.0044$ yields $\phi_c\simeq0.0447$ which, in turn, implies $\phi_{c,R}\equiv\phi_c/\phi_c(\Delta h_p=0)\simeq0.0894$.]

### D. Osmotic pressure Π and the second osmotic virial coefficient $A_2$

Substantial particle clustering is intrinsically reflected in a slow variation of the osmotic pressure Π with the concentration of the associating particle species $\phi_1^o$. Notably, peculiarly ''flat'' curves describing the concentration dependence of Π in the one phase region have been found for the I model.[3] Calculations for the other polymerization models exhibit the same trend, except that the absence of a sharply defined cpc in the F and $A_{high}$ models induces a more gradual increase in Π with $\phi_1^o$, rather than the abrupt ''transition'' to a regime where Π is slowly varying with $\phi_1^o$. Apart from the abruptness of the transition, the ''flattening'' of Π is qualitatively similar in all the models. This crossover in the behavior of Π affects, however, the osmotic compressibility.[3] The abrupt transition of Π to a plateau in $\phi_1^o$ near the cpc in the I model translates into a peak in the osmotic compressibility coefficient,[3] but the rounded nature of the polymerization transition in the F and $A_{high}$ models diminishes this effect. The particle clustering also exerts a particularly strong influence on the second virial coefficient $A_2$, whose magnitude reflects a strong interplay between the short-range van der Waals interaction (characterized by $\epsilon_{FH}$) and the association interaction (specified by $\Delta h_p$, $\Delta s_p$, $\Delta h_a$, $\Delta s_a$). As shown in Paper III, even the sign of $A_2$ cannot be determined from knowledge of $\epsilon_{FH}$ alone, so that substantial renormalization of the ''solvent quality'' (as measured by $A_2$) may arise from association. The present paper analyzes how $\Delta h_p$ and the details of polymerization model influence the $T$ dependence of $A_2$.

A decrease of $\Delta h_p$ is found to produce a successively increased nonlinearity of $A_2(T)$ as a function of $1/T$. This behavior is common to all the models considered and is illustrated for the example of the F model in Fig. 9(a). [In the absence of polymerization, $A_2$ is strictly linear in $1/T$—see Eq. (30)—and this case is included for reference in Fig. 9(a).] The sensitivity of the T dependence of $A_2$ to the model

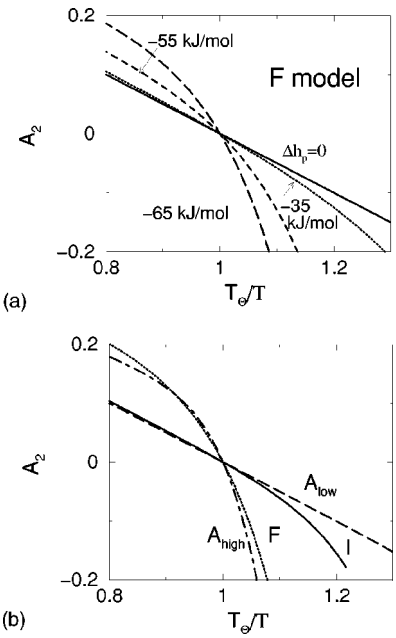


FIG. 9. (a) The dimensionless second osmotic virial coefficient $A_2$ as a function of the reciprocal of the reduced temperature $T_\theta/T$ (where $T_\theta$ is the theta temperature) for the F model. Different curves correspond to different values of the polymerization enthalpy $\Delta h_p$ and are labeled by values of $\Delta h_p$. The strength $\epsilon_{\mathrm{FH}}$ of effective van der Waals monomer–solvent interaction is fixed as $\epsilon_{\mathrm{FH}} \simeq 302$ K. (b) The temperature dependence of $A_2$ for the F, I, $A_{low}$, and $A_{high}$ models. The same polymerization enthalpy ($\Delta h_p = -70$ kJ/mol) and the same strength of effective van der Waals monomer–solvent interaction ($\epsilon_{\mathrm{FH}} \simeq 302$ K) are used for these models.

of polymerization is displayed in Fig. 9(b), which presents $A_2$ as a function of the ratio $T_\theta/T$ for the F, I, $A_{low}$, and $A_{high}$ models. (The theta temperature $T_\theta$ corresponds to the temperature at which $A_2=0$). The enthalpy of polymerization $\Delta h_p$ is chosen in Fig. 9(b) as $\Delta h_p = -70$ kJ/mol in order to enhance the differences between these four models, while all other free energy parameters are the same as in the prior figures. A strong and nonlinear variation of $A_2$ with $1/T$ (both above and below $T_\theta$) for the F and $A_{high}$ models contrasts with the weaker and linear $1/T$ behavior of $A_2$ for the $A_{high}$ and I models. As a matter of fact, $A_2$ in the I model varies linearly with $1/T$ only for $T > T_\theta$, while noticeable deviations from linearity appear for $T < T_\theta$. This finding accords with our prior results for the I model.[3] No deviations from linearity are found for the $A_{low}$ model for which the $T$ dependence of $A_2$ resembles that for a monomer–solvent system. The explanation of this behavior of $A_2$ for the $A_{low}$ model follows simply from Eqs. (51) and (60). Substituting $\Delta h_a = 0$, $\Delta s_a = \Delta s_p = -105$ J/(mol K), and $\Delta h_p = -70$ kJ/mol into Eq. (60) implies that the term $CG_p^2/(1+K_a)^2$, which is the association contribution to $A_2$ in Eq. (60), becomes negligible at high temperatures (say, within $\pm 20\%$ of $T_\theta$). The sensitivity of $A_2$ and other solution properties (e.g., $\Pi$, compressibility factor, etc.) to the model type and strength of the interactions can potentially be used to identify the mechanism of polymerization and the interaction parameters governing the polymerization process.

## VI. DISCUSSION

While the thermodynamics of solutions undergoing equilibrium polymerization exhibit broadly similar patterns, the constraints of thermal activation and chemical initiation exert an appreciable influence on the sharpness and location of the polymerization transition. To gain insights into the *differences* between these basic models of molecular self-organization, we consider many thermodynamic properties of experimental interest, including the average chain length $L$, extent polymerization $\Phi$, Helmhotz free energy $F$, configurational entropy $S$, specific heat $C_V$, polymerization transition temperature $T_p$, osmotic pressure $\Pi$, the second and third osmotic virial coefficients $A_2$ and $A_3$, and the critical temperature $T_c$ and critical composition $\phi_c$. In addition, activation and initiation significantly affect the competition between the phase stability and polymerization and regulate the mass distribution of the polymer clusters. The polymerization transition becomes broad for the ''free association'' model where all monomers *can* associate without restriction, but the transition is narrow at low initiator concentrations or when the activation equilbrium constant is small near the polymerization transition temperature $T_p$. Chain stiffness alters the position of the transition, but the dominant influence of stiffness can generally be absorbed into the definition of the entropy of polymerization. While chemically initiated living polymerization occurs exclusively by adding individual monomers, chains can also form (or break) through chain coupling (or scission) in both the free association and activated association systems, and the thermodynamic properties of these systems are *completely insensitive* to the details of the chain scission and fusion processes. The location of the polymerization transition is found to be highly model dependent and often greatly different from the commonly used Dainton–Ivin equation classical estimate of the polymerization transition temperature. Thus, the maximum in the specific heat $C_V$ and the inflection point in the extent of polymerization $\Phi$ can occur at quite different temperatures for some of the models. In particular, we find that the deviations between these two characteristic temperatures provide a direct measure of the extent of transition rounding in the activated polymerization model, while these temperatures coincide generally for the chemical initiation model.

The competition between phase separation and polymerization is examined by analyzing the influence of the enthalpy $\Delta h_p$ and entropy $\Delta s_p$ of polymerization and the strength $\epsilon_{\mathrm{FH}}$ of the effective monomer–solvent van der Waals interaction ($\chi = \epsilon_{\mathrm{FH}}/T$) on the critical temperature $T_c$ and critical composition $\phi_c$. For a given polymerization model, both $T_c$ and $\phi_c$, normalized by their values in the absence of polymerization, are functions of the dimensionless ''sticking energy'' $h_\epsilon \equiv (|\Delta h_p|/R)/(2\epsilon_{\mathrm{FH}})$ and of $\Delta s_p$. In general, $T_c(h_\epsilon)/T_c(h_\epsilon=0)$ increases monotonically and sigmoidally with $h_\epsilon$ and the rate of this increase is controlled by $\Delta s_p$. The variation of the reduced critical temperature with $h_\epsilon$ is characterized by two critical values of $h_\epsilon$: at the first ($h_{\epsilon,1}$) this ratio starts growing from unity, and it saturates at the second ($h_{\epsilon,2}$) to a limiting value related to the theta teperature $T_\theta$ ($A_2=0$) of the polymer fluid. When the polymerization transition is ''close'' to being second order,

*two* critical points are present over a certain range of $h_\epsilon$. Transition rounding in the thermally activated and chemically initiated models, however, causes the disappearance of these multiple critical points.

Our analysis of various thermodynamic properties in Sec. V is designed to compare and contrast the three basic models of equilibrium polymerization: the free association, chemical initiation, and thermally activated association models. While the first two models are completely characterized by the enthalpy $\Delta h_p$ and entropy $\Delta s_p$ of polymerization (and by $r$ in the case of the I model[48]), several variants of the activated association model are possible, depending on whether activated or unactivated monomers participate in the chain propagation steps. Thus, two different activated polymerization mechanisms are considered in Sec. III. In the first reaction scheme, the activated species $M_1^*$ reacts only with unactivated monomers $M_1$ (to form dimers), but does not react with other species $M_i$ $(i>2)$ to form higher order polymers [see Eqs. (36)–(38)]. Alternatively, in the second scheme, the activated monomers $M_1^*$ participate in both the dimerization and chain propagation processes [see Eqs. (40) and (41)]. As noted earlier, these two activation models are mathematically isomorphic, i.e., become identical upon introducing an appropriate redefinition of the corresponding free energy parameters [see Eqs. (62) and (63)]. Hence, our comparison of basic models of equilibrium polymerization is performed for the first activation model defined by Eqs. (36)–(38). Since the behavior of the activation model varies strongly with the activation free energy, we distingush three activation models $A_{low} \equiv A(K_a = 3.28\times 10^{-6})$, $A_{high} \equiv A(K_a = 3.28\times 10^{-6}\exp(4210/T))$, and $A_{int} \equiv A(K_a = 3.28\times 10^{-6}\exp(2105/T))$ corresponding to a low, high, and intermediate values of the activation equilibrium constant $K_a$, respectively, at $T=T_p$. Other mechanisms than those illustrated by Eqs. (36)–(38) and (39)–(41) are also possible [for instance, a mechanism based on a combination of Eqs. (36) and (37) with Eq. (41)]. In addition, different equilibrium constants may be assigned to the dimerization and the chain propagation steps, as is necessary, for instance, to describe experimental data for the polymerization of G-actin.[38] However, to keep the number of free energy parameters to a minimum, these processes are assumed here to be governed by the same $\Delta h_p$ and $\Delta s_p$.

The comparison of the equilibrium polymerization models in Sec. V is carried out for the same enthalpy $\Delta h_p = -35$ kJ/mol and entropy $\Delta s_p = -105$ J/(mol K) of polymerization. The choice of negative $\Delta h_p$ and $\Delta s_p$ restricts attention to systems that polymerize upon cooling. The theory, of course, also applies to systems that polymerize upon heating $(\Delta h_p>0, \Delta s_p>0)$ and their behavior is somewhat richer due to the presence of multiple (lower and upper) critical points in the phase diagrams for some of these systems.[1,49]

Some of the thermodynamic characteristics of the polymerization models are quite specific for the model involved. For instance, the rate at which the average degree of polymerization $L$ varies with temperature and even the limiting low temperature value of $L(T)$ are model dependent. The concentration dependence of $L$ is not universal either, ranging from a linear dependence for the I and $A_{low}$ models to a $(\phi_1^o)^{1/2}$ scaling for the F, $A_{int}$, and $A_{high}$ models. The magnitude of $L$ at the polymerization transition temperature $T_p$ is nearly insensitive to $\phi_1^o$ and remains close to unity in all the models considered, except for the F model where $L_p \simeq 3$. Both $L$ and the extent of polymerization $\Phi$ may become nonmonotonic functions of temperature and exhibit maxima due to the competition between polymerization and activation processes. Substantial deviations of $T_p$ from the Dainton–Ivin equation emerge for the F and $A_{high}$ model and imply that this simple and widely used equation is generally unreliable for estimating the polymerization parameters $(\Delta h_p, \Delta s_p)$ from experimental data for $T_p$. The specific heat $C_V(T)$ curves (see Fig. 3) and polymerization lines $T_p(\phi_1^o)$ [see Fig. 4(a)] confirm the similarity between the I and $A_{low}$ models as evidenced by Figs. 1 and 2 and characterized by a sharp polymerization transition for these models. On the other hand, the polymerization is very broad in the F model.

All these particular characteristics of the polymerization models are helpful in discriminating the type of polymerization process that occurs in any given physical system. For example, it has been suggested that equilibrium polymerization describes the formation of worm-like micelles in nonionic surfactants, such as lecithin water–oil microemulsions and hexaethylene glycol *n*-hexadecyl monoether in water.[24,50,51] In both of these model nonionic systems, the average chain length scales in near proportion to the monomer concentration rather than the ''expected'' 1/2 power.[50] Moreover, these systems exhibit evidence of a well-defined maximum in the inverse osmotic compressibility (and in the static and dynamic correlation lengths at nearly the same ''overlap'' concentations).[50,51] The near linear concentation dependence of $L(\phi_1^o)$ and the maximum in the ''osmotic modulus'' are characteristic features of equilibrium polymerization with thermal activation. Although the formation of spherical micelles proceeds by a self-assembly process that differs from those considered here because of geometric packing constraints, the aggregation of spherical micelles into worm-like polymers can perhaps be treated as an activated equilbrium polymerization process. At any rate, the experimental observations[50,51] strongly suggest that the F model is inadequate to describe worm-like micelle formation, while the $A_{low}$ model seems to be quite compatible. The F model might be quite useful, however, for treatments of surfactant systems in which the degree of thermal activation is high. Our generalized thermodynamic models of equilibrium polymerization thus point the way toward formulating physically more accurate models of polymerization processes that occur in real complex fluid systems.

As already mentioned, the dependence of the critical parameters ($T_c$ and $\phi_c$) on the enthalpy of polymerization $\Delta h_p$ and on the strength $\epsilon_{FH}$ of the effective monomer–solvent van der Waals interaction also differs between the various models [see Figs. 6(a) and 8]. A limited extent of polymerization in the $A_{high}$ model causes $T_c$ and $\phi_c$ to become practically insensitive to the dimensionless interaction $h_\epsilon \equiv (|\Delta h_p|/R)/(2\epsilon_{FH})$. The gradual polymerization transition in the F model is responsible for a slower variation of $T_c$ and $\phi_c$ with $h_\epsilon$ than in the I and $A_{low}$ models. Remarkably, $T_c$ in

all the models never exceeds the theta temperature $T_\theta$ for the unpolymerized monomer–solvent systems, thereby providing a fundamental limit to the critical temperature for arbitrary $h_\epsilon$. Another interesting aspect of critical phenomena in equilibrium polymerization solutions lies in the presence of two critical points in the phase diagram for the I and $A_{low}$ models [see Fig. 6(b)]. The first critical point ($T_c = \epsilon_{FH}/2$, $\phi_c = 1/2$) is evidently reminiscent of the critical point for an unpolymerized monomer–solvent system, whereas the second critical point emerges due to the presence of a sharp polymerization transition. Two critical points do not occur in the F, $A_{int}$, or $A_{high}$ models where the transition is highly ''rounded.'' [52] A similar pattern of critical behavior to those described here for the I and $A_{low}$ models has been found in theoretical studies of associating fluids that form branched polymers.[53] Specifically, the mean field (Cayley tree) calculations of Tanaka and Matsuyama[53] indicate the occurrence of a sharp polymerization transition and two critical points for a limited range of $\Delta h_p$. Thus, it may be concluded that the formation of branched structures leads to a ''sharpening'' (decreased rounding) of the clustering transition since the polymerization transition is very broad in the F model (corresponding to bifunctional association in the model of Tanaka and Matsuyama[53]). We plan to investigate equilibrium branched polymers using the lattice model approach of the present paper to understand this nonintuitive phenomenon. An extension of the F model to branched polymer systems might also be relevant to descriptions of thermoreversible gelation.[54]

## ACKNOWLEDGMENT

This work was partially performed under the sponsorship of the U.S. Department of Commerce, National Institute of Standards and Technology.

## APPENDIX: LOW TEMPERATURE SCALING OF $L$ AND $\phi_c$ IN THE FREE ASSOCIATION MODEL

The relationship between $L$ and $\Phi$ is specified by Eq. (27) as

$$L = \frac{2-A}{2-A-\Phi}, \quad 0<\Phi<1, \quad 0<A<1, \tag{A1}$$

where $\Phi$ and $A$ are defined as

$$\Phi = 1-\phi_1/\phi_1^o, \quad A = \phi_1 G, \tag{A2}$$

$G \equiv \alpha \exp(-\Delta f_p/k_B T)$, $\Delta f_p$ is the free energy of polymerization, and the coefficient $\alpha$ equals $(z-1)$ and 1 for fully flexible chains and for stiff chains, respectively.

Consider polymerization upon cooling, i.e., limit our discussion to $\Delta h_p<0$, $\Delta s_p<0$. In the low temperature regime ($T \ll T_p$) where $G \gg 1$, the concentration of unreacted monomers $\phi_1 \to 0$, the fraction of polymerized monomers $\Phi \to 1$, and the average chain length $L$ becomes large ($L \gg 1$). Consequently, $A$ approaches unity [see Eq. (A1)] and may be formally expressed as

$$A(T \ll T_p) = 1-\epsilon, \quad \epsilon \to 0^+, \tag{A3}$$

where $\epsilon$ is positive and small. Substituting Eqs. (A2) and (A3) into Eq. (A1) yields

$$L(T \ll T_p) = \frac{1}{\epsilon} + O(\epsilon^{-2}). \tag{A4}$$

On the other hand, $\epsilon$ can be determined from the mass conservation Eq. (19),

$$\phi_1^o = \phi_1 + \frac{CA^2(2-A)}{(1-A)^2}, \quad C = \frac{z}{2\alpha G}. \tag{A5}$$

Replacing $\phi_1$ in Eq. (A5) by $A/G$ and $A$ by $(1-\epsilon)$ and ignoring cubic terms in $\epsilon$ in the resulting equation lead to the quadratic form,

$$[1+(G\phi_1^o-1)(2\alpha/z)]\epsilon^2 + \epsilon - 1 = 0, \tag{A6}$$

which can be solved for $\epsilon$,

$$\begin{aligned}\epsilon &= \frac{-1+\sqrt{1+4[1+(G\phi_1^o-1)(2\alpha/z)]}}{2[1+(G\phi_1^o-1)(2\alpha/z)]} \\ &\simeq \sqrt{\frac{1}{G\phi_1^o(2\alpha/z)}} \\ &= \sqrt{\frac{C}{\phi_1^o}}.\end{aligned} \tag{A7}$$

Thus, the asymptotic average polymerization index is

$$L(T \ll T_p) \simeq \frac{1}{\epsilon} \simeq \sqrt{G\phi_1^o(2\alpha/z)} = \sqrt{\frac{\phi_1^o}{C}}. \tag{A8}$$

The critical composition $\phi_c$ for the free association system is defined through the condition,

$$\left.\frac{\partial^3 F/(N_l k_B T)}{\partial(\phi_1^o)^3}\right|_{N_l, T=T_c} = 0. \tag{A9}$$

Reexpressing the third derivative of $F$ with respect to $\phi_1^o$ in terms of $\epsilon = (C/\phi_1^o)^{1/2}$ [see Eq. (A7)] transforms the condition in Eq. (A9) into a simple polynomial,

$$b\phi_c^{5/2} - \phi_c^2 + 2\phi_c - 1 = 0, \tag{A10}$$

where $b \equiv 4/(3\sqrt{C_{cr}})$ and $C_{cr} = z/(2\alpha \exp[-\Delta f/k_B T_c])$. Since $\phi_c \ll 1$ and $b \gg 1$, the linear and quadratic terms in $\phi_c$ can be neglected in Eq. (A10), leading to the solution,

$$\begin{aligned}&\phi_c \simeq \left(\frac{3}{4}\right)^{2/5}\left[\frac{z}{2\alpha \exp[-\Delta f/(2k_B\epsilon_{FH})]}\right]^{1/5}, \\ &\Delta h_p<0, \quad \Delta s_p<0, \quad T_c \ll T_p.\end{aligned} \tag{A11}$$

[1] J. Dudowicz, K. F. Freed, and J. F. Douglas, J. Chem. Phys. **111**, 7116 (1999) (Paper I).
[2] J. Dudowicz, K. F. Freed, and J. F. Douglas, J. Chem. Phys. **112**, 1002 (2000) (Paper II).
[3] J. Dudowicz, K. F. Freed, and J. F. Douglas, J. Chem. Phys. **113**, 434 (2000) (Paper III).
[4] S. C. Greer, J. Phys. Chem. B **102**, 5413 (1998).
[5] S. C. Greer, Adv. Chem. Phys. **94**, 261 (1996).
[6] J. Dudowicz, K. F. Freed, and J. F. Douglas (unpublished).
[7] F. Dolezalek, Z. Phys. Chem. **64**, 727 (1908).
[8] M. E. Fisher and D. M. Zuckerman, J. Chem. Phys. **109**, 7961 (1998).
[9] G. Gee, Trans. Faraday Soc. **48**, 515 (1952); Sci. Prog. **170**, 193 (1955).

[10] A. V. Tobolsky and A. Eisenberg, J. Am. Chem. Soc. **81**, 780 (1959).
[11] A. V. Tobolsky and A. Eisenberg, J. Colloid Sci. **17**, 49 (1962); J. Am. Chem. Soc. **82**, 289 (1960); **81**, 2302 (1959); A. V. Tobolsky, A. Rembaum, and A. Eisenberg, J. Polym. Sci. **45**, 345 (1960); A. V. Tobolsky, *ibid.* **25**, 220 (1957).
[12] R. G. Petschek, P. Pfeuty, and J. C. Wheeler, Phys. Rev. A **34**, 2391 (1986).
[13] I. G. Economou and M. D. Donohue, AIChE J. **37**, 1875 (1991).
[14] G. Jackson, W. G. Chapman, and K. E. Gubbins, Mol. Phys. **65**, 1 (1988).
[15] A. Milchev and D. P. Landau, Phys. Rev. E **52**, 6431 (1995); J. Chem. Phys. **104**, 9161 (1996).
[16] J. P. Wittmer, A. Milchev, and M. E. Cates, J. Chem. Phys. **109**, 834 (1998).
[17] S. J. Kennedy and J. C. Wheeler, J. Chem. Phys. **78**, 953 (1983).
[18] J. C. Wheeler, S. J. Kennedy, and P. Pfeuty, Phys. Rev. Lett. **45**, 1748 (1980); J. C. Wheeler and P. Pfeuty, Phys. Rev. A **24**, 1050 (1981).
[19] S. J. Kennedy and J. C. Wheeler, J. Chem. Phys. **78**, 1523 (1983).
[20] J. C. Wheeler and P. Pfeuty, Phys. Rev. Lett. **46**, 1409 (1981).
[21] J. C. Wheeler, Phys. Rev. Lett. **53**, 174 (1984); J. Chem. Phys. **81**, 3635 (1984).
[22] S. J. Kennedy and J. C. Wheeler, J. Chem. Phys. **78**, 953 (1983).
[23] J. P. Wittmer, A. Milchev, and M. E. Cates, Europhys. Lett. **41**, 291 (1998).
[24] M. E. Cates and S. J. Candau, J. Phys.: Condens. Matter **2**, 6892 (1990).
[25] R. Scott, J. Chem. Phys. **69**, 261 (1965).
[26] J. Dudowicz, K. F. Freed, and J. F. Douglas, Phys. Rev. Lett. (in press).
[27] P. J. Flory, *Principles of Polymer Chemistry* (Cornell University Press, Ithaca, 1953).
[28] J. Dudowicz and K. F. Freed, Macromolecules **24**, 5076 (1991).
[29] J. T. Kindt and W. M. Gelbart, J. Chem. Phys. **114**, 1432 (2001).
[30] H. Rahage and H. Hoffmann, Mol. Phys. **74**, 933 (1991).
[31] S. Bastea, Phys. Rev. E **66**, 020801 (2002).
[32] J. Dudowicz, K. F. Freed, and J. F. Douglas (unpublished).
[33] F. S. Dainton and K. J. Ivin, Nature (London) **162**, 705 (1948).
[34] S. C. Greer, Annu. Rev. Phys. Chem. **53**, 173 (2002).
[35] Y. B. Melnichenko, G. D. Wignall, and W. A. Van Hook, Europhys. Lett. **48**, 372 (1999); P. Debye, H. Coll, and D. Woermann, J. Chem. Phys. **33**, 1746 (1960).
[36] F. Oosawa and S. Asakura, *Thermodynamics of Polymerization of Protein* (Academic, New York, 1975).
[37] A second critical point with $\phi_c > 0.5$ may appear in the activated association model over a limited range of $\Delta h_p$.
[38] P. S. Niranjan, P. B. Yim, J. G. Forbes, S. C. Greer, J. Dudowicz, K. F. Freed, and J. F. Douglas, J. Chem. Phys. **119**, 4070 (2003).
[39] F. W. Starr, J. F. Douglas, and S. C. Glotzer, J. Chem. Phys. **119**, 1777 (2003).
[40] I. Prigogine and R. Defay, *Chemical Thermodynamics* (Longmans, London, 1954).
[41] Recent measurements of nonionic micelle forming liquids (for which living polymerization is thought to be an appropriate model) indicate a nearly linear dependence of $L$ on the associating species (surfactant) concentration $\phi_1^o$. See P. Schurtenberger and C. Cavaco, J. Phys. II **3**, 1279 (1993); **4**, 395 (1994); G. J. M. Koper, C. Cavaco, and P. Schurtenberger, in *25 Years of Non-Equilibrium Thermodynamics*, edited by J. J. Brey, J. Marro, J. M. Rubi, and M. San Miguel (Springer, Verlag, Berlin, 1995), p. 363; P. Schurtenberger *et al.*, Langmuir **12**, 2894 (1996).
[42] P. S. Niranjan, J. G. Forbes, S. C. Greer, J. Dudowicz, K. F. Freed, and J. F. Douglas, J. Chem. Phys. **114**, 10573 (2001).
[43] R. Ivkov, J. G. Forbes, and S. C. Greer, J. Chem. Phys. **108**, 5599 (1998).
[44] Although our previous attempts to determine $T_c$ from Eqs. (3) and (10)–(12) of Paper II encountered numerical instabilities for small $\epsilon_{\mathrm{FH}}$, the analysis of Eq. (89) demonstrates that $T_c$ exists for all positive $\epsilon_{\mathrm{FH}}$.
[45] Notice that the sticking energy $h_\epsilon^* = 3.32$ departs only slightly from $h_{\epsilon,1} = 3.16$.
[46] K. M. Zheng, S. C. Greer, L. R. Corrales, and J. Ruiz-Garcia, J. Chem. Phys. **98**, 9873 (1993) provide a summary of the critical phenomena in equilibrium polymer solutions.
[47] J. Dudowicz, K. F. Freed, and J. F. Douglas (unpublished).
[48] The full description of the I model must also involve specification of the number of initiator molecules in each polymer. Equations (64) and (65) apply to system where all polymers contain two initiator molecules.
[49] Scott (Ref. 25) and Wheeler and co-workers (Refs. 18 and 19) have discussed the thermodynamic properties of sulfur, which is a typical example of systems that polymerize upon heating.
[50] P. Schurtenberger, C. Cavaco, F. Tiberg, and O. Regev, Langmuir **12**, 2894 (1996).
[51] P. Schurtenberger and C. Cavaco, J. Phys. II **4**, 305 (1994); **3**, 1279 (1993); Langmuir **10**, 100 (1994).
[52] Our equilibrium polymerization model also predicts the existence of multiple critical points in one component associating fluids, where the polymerization transition is nearly a second-order transition. A "liquid–liquid" transition between predominantly monomeric and polymeric liquid phases has been reported in pure phosphorous and carbon. The appearance of two critical points has also been found for supercooled water, silica, $SiO_2$, $GeO_2$, Ge, Bi, Se, or Te. [See G. Malescio, G. Franzese, G. Pellicane, A. Skibinsky, S. V. Buldyrev, and H. E. Stanley, J. Phys.: Condens. Matter **14**, 2193 (2002) and Y. Katayama, T. Mizutani, W. Utsumi, O. Shimomura, M. Yamakata, and K. Funakoshi, Nature (London) **403**, 170 (2000)].
[53] F. Tanaka and A. Matsuyama, Phys. Rev. Lett. **62**, 2759 (1989).
[54] P. Varadan and M. J. Solomon, Langmuir **19**, 509 (2003); M. C. Grant and W. B. Russel, Phys. Rev. E **47**, 2606 (1993); A. T. J. M. Woutersen and C. G. de Kruif, J. Chem. Phys. **94**, 5739 (1991).